



**University of Dundee**

**A new approach for determination of free carriers lifetime and density of localised states in disordered semiconductors**

Belgacem, Hocine; Reynolds, Stephen

*Published in:*  
Philosophical Magazine

*DOI:*  
[10.1080/14786435.2018.1532120](https://doi.org/10.1080/14786435.2018.1532120)

*Publication date:*  
2019

*Document Version*  
Peer reviewed version

[Link to publication in Discovery Research Portal](#)

*Citation for published version (APA):*  
Belgacem, H., & Reynolds, S. (2019). A new approach for determination of free carriers lifetime and density of localised states in disordered semiconductors. *Philosophical Magazine*, 99(2), 131-147.  
<https://doi.org/10.1080/14786435.2018.1532120>

**General rights**

Copyright and moral rights for the publications made accessible in Discovery Research Portal are retained by the authors and/or other copyright owners and it is a condition of accessing publications that users recognise and abide by the legal requirements associated with these rights.

- Users may download and print one copy of any publication from Discovery Research Portal for the purpose of private study or research.
- You may not further distribute the material or use it for any profit-making activity or commercial gain.
- You may freely distribute the URL identifying the publication in the public portal.

**Take down policy**

If you believe that this document breaches copyright please contact us providing details, and we will remove access to the work immediately and investigate your claim.



**A new approach for determination of free carriers lifetime and density of localized states in disordered semiconductors**

|                               |   |
|-------------------------------|---|
| Journal:                      | <i>Philosophical Magazine &amp; Philosophical Magazine Letters</i>  |
| Manuscript ID                 | TPHL-18-Jun-0063.R1   |
| Journal Selection:            | Philosophical Magazine  |
| Date Submitted by the Author: | 08-Sep-2018   |
| Complete List of Authors:     | Belgacem, Hocine; Faculty of Matter Science, University Hadj Lakhdar Batna 1, Department of Physics<br>Reynolds, Stephen; University of Dundee, Electronic Engineering and Physics; |
| Keywords:                     | a-Si:H, amorphous semiconductors, electronic density of states, electronic properties, localized states, materials characterisation, thin films, transport properties               |
| Keywords (user supplied):     | Transient Photocurrent, Recombination lifetime, Laplace transform   |
|                               |   |

SCHOLARONE™  
Manuscripts

1  
2 A new approach for determination of free carriers lifetime and density of localized states in  
3  
4 disordered semiconductors

5  
6 H. Belgacem<sup>a,\*</sup>, S. Reynolds<sup>b</sup>  
7  
8  
9

10  
11 <sup>a</sup> *Department of Physics, Faculty of Matter Science, University Hadj Lakhdar Batna 1, 5 avenue Chahid*  
12  
13 *Boukhlouf, 05000 Batna, Algeria*

14  
15 <sup>b</sup> *Physics Division, School of Engineering, Physics and Mathematics, University of Dundee, Dundee DD1 4HN,*  
16  
17 *UK*  
18  
19  
20

21 **Abstract**

22  
23 A new method for measuring the free carriers lifetime ( $\tau_R$ ) and the density of localized  
24 states (DOS) in amorphous semiconductors is described. The method is based on the analysis  
25 of transient photoconductivity (TPC) data using Laplace transform technique. This technique  
26 involves Laplace transform of TPC data, it is a simple analysis of the solution of the basic  
27 linearized multiple trapping equations for free and trapped electrons. It is demonstrated by  
28 application to simulated and experimental TPC data measured on a typical disordered  
29 semiconductor, the hydrogenated amorphous silicon (a-Si:H). An introduced  $\tau_R$  in the  
30 computing of the TPC using an arbitrarily proposed DOS model is recovered with high  
31 accuracy. For the experimental case, the determination of the exact DOS and the estimated  $\tau_R$   
32 from the experimental TPC data allow to reconstruct accurately this last. The performance  
33 and limitations of the technique are studied by means of computer simulations. Limitations  
34 are essentially the low temperatures of measurement of TPC when the recombination  
35 phenomenon is not observed at short times.  
36  
37  
38  
39  
40  
41  
42  
43  
44  
45  
46  
47  
48  
49  
50  
51  
52  
53

54  
55  
56 *Keywords: Transient Photocurrent; Recombination lifetime; DOS; Laplace transform*

57  
58 <sup>\*</sup> Corresponding author. Tel.: +213 6 62296115; fax: +213 33 319017.

59  
60 *E-mail address: hocine.belgacem@univ-batna.dz (H. Belgacem).*

## 1. Introduction

Photodecay decay experiments have been used to measure the recombination lifetime of photogenerated carriers in semiconductors [1]. In amorphous semiconductors, the TPC decay experiments also enable us to determine the characteristic recombination time  $\tau_c$  from the transition point from the pre-transit photocurrent  $I_{ph}$  vary as  $t^{-(1-\alpha)}$  to the post-transit one vary as  $t^{-(1+\alpha)}$  in case of the monomolecular recombination process [2] and by assuming an exponential decreasing density of localized states  $g(E) = g(E_c) \exp\left(\frac{-E}{kT_c}\right)$ , where  $\alpha = \frac{T}{T_c}$  for  $T < T_c$  is the dispersion parameter. Transitions to the post-transit region occur at various times, increasing with increasing  $\tau_R$ . The  $\tau_c$  can be related to  $\tau_R$  by assuming the thermalization of photogenerated carriers into an exponential band tail of localized defects [2]. However, the precise measurement of  $\tau_c$  suffers from the gradual transitions in the photocurrent from  $I_{ph} \propto t^{-(1-\alpha)}$  to  $I_{ph} \propto t^{-(1+\alpha)}$ . In addition, it has been shown that the thermalization approximation does not work for structured distributions of localized tail states [3] and for exponential band tail states whose width is smaller than  $kT$ , where  $kT$  is the thermal energy. Information on  $\tau_R$  is important for the understanding of nature of recombination centers in amorphous semiconductors. Since the transient photocurrent is intimately related to the energetic distribution of localized states and  $\tau_R$ , it may be used to study them, and various techniques have been advanced for doing so [4-6]. The DOS and  $\tau_R$  are key material quality indicators, of importance in the design of improved solar cells, photodetectors and thin-film transistors. A simple and reliable method is introduced to evaluate  $\tau_R$ .

We develop in this paper a new method for measuring  $\tau_R$  and DOS  $g(E)$  in disordered semiconductors from an experimental transient photocurrent data. The present method consists of three steps: first,  $\tau_R$  is estimated from the experimental TPC data using Laplace

transform technique. Secondly, exact DOS  $g(E)$  is determined from the same experimental TPC data using the same Laplace transform technique [7-10]. Thirdly, computer-generated transient photocurrent using the calculated  $\tau_R$  and DOS  $g(E)$  must reproduce the experimental one, and thus to valid the method. The method is applied to the study of the effects of random noise and truncated data on  $\tau_R$  for simulated TPC on the one hand and the effect of temperature on  $\tau_R$  in undoped a-Si: H sample on the other hand.

## 2. Theory

### 2.1. Recombination lifetime determination

In the TPC technique, the transient photocurrent is determined by the time dependence of the photoconductivity following carrier excitation by means of a short pulse of illumination in samples having a coplanar electrode configuration [2]. For the theoretical analysis of this measurement, it suits to assume unipolar conduction, equal capture cross section for all localized states and small signal condition (the injected charge density is low enough that the localized states are not saturated and that the internal electric field is not perturbed) [7]. The small signal condition ensures the monomolecular recombination kinetics of photogenerated carriers and avoids space charge effects. We assume the transient photocurrent is carried solely by carriers in extend states, which interact through trapping and release with a distribution of localized states. Then, the basic linearized multiple trapping equations for free and trapped electrons respectively are:

$$\frac{dn(t)}{dt} = -\sum_i \frac{dn_i(t)}{dt} - \frac{n(t)}{\tau_R} + N_0 \delta(t), \quad (1)$$

$$\frac{dn_i(t)}{dt} = \omega_i n(t) - \gamma_i n_i(t), \quad (2)$$

where  $n(t)$  is the free carrier density at time  $t$ ,  $n_i(t)$  the trapped carrier density at the  $i^{th}$  localized state at time  $t$ ,  $N_0$  the pulsed electron density (the excess free electron density at

the initial time  $t = 0$ ),  $\tau_R$  the recombination lifetime,  $\omega_i = \sigma v g(E_i) \Delta E$  the capture rate constant,  $\gamma_i = \nu \exp\left(\frac{-E_i}{kT}\right)$  the release rate constant,  $E_i = i\Delta E$  the  $i^{\text{th}}$  energy level below (or above) a mobility edge,  $\sigma$  the capture cross section,  $\nu$  the thermal velocity and  $\nu$  the attempt-to-escape frequency. The delta function in Eq. (1) defines the initial condition for the transient photoconductivity experiment. We set the conduction band mobility edge at  $E_c = 0$ , so that  $E$  is negative.

Eqs. (1) and (2) may be solved to yield the Laplace transform of the free carrier density  $n(t)$ . The Laplace transform of  $n(t)$  is defined as:

$$\hat{n}(s) = \int_0^{\infty} n(t) e^{-st} dt$$

The solution of Eqs. (1) and (2) for  $\hat{n}(s)$  is:

$$\hat{n}(s) = \frac{N_0}{s + \frac{1}{\tau_R} + \sum_i \frac{s\omega_i}{s + \gamma_i}}, \quad (3)$$

that is to say

$$\frac{1}{\tau_R} = \frac{N_0}{\hat{n}(s)} - s \left( 1 + \sum_i \frac{\omega_i}{s + \gamma_i} \right), \quad (4)$$

in which  $s$  is the Laplace variable.

For the TPC experiment, the photocurrent is given by  $I(t) = q\mu_0 F S n(t)$ , where  $q$  is the electron charge,  $\mu_0$  the microscopic mobility,  $F$  the applied electric field and  $S$  the conduction cross section, which is transformed into

$$\hat{I}(s) = q\mu_0 F S \hat{n}(s) . \quad (5)$$

Inserting Eq. (5) into Eq. (4), one obtains

$$\frac{1}{\tau_R} = \frac{q\mu_0 F S N_0}{\hat{I}(s)} - s \left( 1 + \sum_i \frac{\omega_i}{s + \gamma_i} \right), \quad (6)$$

for  $s = 0$  one obtains

$$\tau_R = \frac{\hat{I}(0)}{I(0)} = \frac{\int_0^{\infty} I(t) dt}{I(0)}, \quad (7)$$

where  $I(0) = q\mu_0 FSN_0$ , which is estimated from the extrapolated value of  $I(t)$  to  $t = 0$ .

$\hat{I}(0)$  can be carried out by a simple numerical integration over  $N$  sampling points  $t_j$ :

$$\hat{I}(0) = \sum_{j=2}^{N-1} I(t_j) \Delta t_j, \quad (8)$$

where  $\Delta t_j = \frac{t_{j+1} - t_{j-1}}{2}$ .

Eq. (7) is a simple and adequate relationship that leads to the estimate of  $\tau_R$ . Like one sees  $\tau_R$  depends only on experimental  $I(t)$  data and initial photocurrent  $I(0)$ , i.e. generated excess density  $N_0$ .

To investigate the potential accuracy of the  $\tau_R$  determination procedure, it is necessary to simulate accurately the transient photocurrent for the following two representative localized state distributions in amorphous and polymeric semiconductors: (i) an exponential distribution

$g(E) = g(E_c) \exp\left(\frac{-E}{kT_c}\right)$  and (ii) an exponential distribution on which a Gaussian distribution

has been superimposed  $g(E) = g(E_c) \exp\left(\frac{E}{kT_c}\right) + g_g \exp\left[-\left(\frac{E - E_g}{E_w}\right)^2\right]$ , where  $g(E_c)$  is the

density of localized states at the mobility edge,  $T_c$  the characteristic temperature and  $g_g$ ,  $E_g$  and  $E_w$  the peak value, the energy position from the mobility edge and the energy width of the Gaussian distribution, respectively.

In the present work  $n(t)$  was carried out by means of an analytical expression for the inverse Laplace transform of  $\hat{n}(s)$ , obtained from Eq. (3), using Heaviside's expansion theorem [11].

$$n(t) = L^{-1}\{\hat{n}(s)\} = \sum_{i=1}^{n+1} \frac{P(\alpha_i)}{Q'(\alpha_i)} e^{\alpha_i t}, \quad (9)$$

In Eq. (9) the  $\alpha_i$  are the  $n+1$  zeroes of the denominator  $Q(s)$  and  $Q'(\alpha_i)$  is the first derivative of  $Q(s)$  taken at points  $\alpha_i$ .  $\hat{n}(s)$  is of the form of  $\frac{P(s)}{Q(s)}$ .

Fig. 1b shows the TPC,  $n(t)$ , computed at 300K for the proposed exponential DOS model of Fig. 1a with various values of  $\tau_R$ . The inflection points in the transients are due to the monomolecular recombination of the photogenerated free carriers. The characteristic recombination time determined from the inflection point,  $\tau_c$ , is much larger than  $\tau_R$ , this results from frequent trapping and detrapping of free carriers into the exponential localized-state distributions. The value of  $\tau_c$  increases with  $\tau_R$ . The  $\tau_R$  used in the simulation of  $n(t)$ , are, respectively,  $10^{-8}$ ,  $10^{-7}$  and  $10^{-6}$  s. The corresponding calculated  $\tau_R$  using Eq. (7) are, respectively,  $9.0165 \times 10^{-9}$ ,  $8.8164 \times 10^{-8}$  and  $8.7647 \times 10^{-7}$  s. It can be seen that the introduced  $\tau_R$  were recovered with high accuracy.

Fig. 2b shows the TPC,  $n(t)$ , computed at 350K for the proposed exponential plus Gaussian DOS model of Fig. 2a with  $\tau_R = 10^{-8}$  s. As in the case of computed TPC,  $n(t)$ , for an exponential DOS model, One can see well the inflection point in the transient due to recombination. The corresponding calculated  $\tau_R$  using Eq. (7) is  $8.7256 \times 10^{-9}$  s. It can be seen here also that the proposed method recovers very precisely the introduced  $\tau_R$ .

Figs. 3a, 3b, 3c and 4 show the TPC,  $n(t)$  (symbol), of Figs. 1b ( $\tau_R = 10^{-6}, 10^{-7}, 10^{-8}$  s) and 2b respectively, and  $\tau_R(s^{-1})$  (solid line) for corresponding  $\hat{n}(s)$  (Eq. (4)). One can see that  $\tau_R(s^{-1})$  remains constant till the characteristic recombination time  $\tau_c$  and equal to introduced value of  $\tau_R$  in the simulation of  $n(t)$ . Normally  $\tau_R$  is independent of  $s$ , but most important is that  $\tau_R(s^{-1})$  is constant and equal to introduced  $\tau_R$  for small values of  $s$  and for



1  
2  
3  
4  
5  
6  
7  
8  
9  
10  
11  
12  
13  
14  
15  
16  
17  
18  
19  
20  
21  
22  
23  
24  
25  
26  
27  
28  
29  
30  
31  
32  
33  
34  
35  
36  
37  
38  
39  
40  
41  
42  
43  
44  
45  
46  
47  
48  
49  
50  
51  
52  
53  
54  
55  
56  
57  
58  
59  
60

$s = 0$  also of course (Eq. (7)). An important observation, the curve  $\tau_R(s^{-1})$  deviates from introduced  $\tau_R$  exactly at the moment when recombination begins, the curves  $n(t)$  and  $\tau_R(s^{-1})$  intersect at this specific time. Which means that the proposed method is not valid when the recombination phenomenon is not observed, this happens for low temperatures of measurement of  $n(t)$ , at short times.

## 2.2. Density of localized states

Eq. (6) can also be written as follows:

$$\sum_i \frac{g(E_i)}{s + \gamma_i} = \frac{1}{s \sigma v \Delta E} \left( \frac{q \mu_0 F S N_0}{\hat{I}(s)} - s - \frac{1}{\tau_R} \right), \quad (10)$$

We note here  $\tau_R$  is experimentally known (Eq. (7)).

Eq. (10) is an integro-differential equation for the DOS  $g(E)$ , termed a Fredholm integral equation of the first kind [12] which may arise from an ‘ill-conditioned problem’. The inversion of this equation to obtain the DOS requires care, it needs a special resolution method. The resolution method used here is an exact matrix solution for  $g(E)$  based on Tikhonov regularization [13,14]. Written in a discrete form, Eq. (10) yields

$$\sum_{i=1}^M g(i) A(j, i) = b(j) \quad \text{for } j = 2, \dots, N-1, \quad (11)$$

where  $i$  and  $j$  are the energy and time indexes respectively, and  $g(i) = g(E_i)$ . The matrix elements  $A(j, i)$  and the vector elements  $b(j)$  are respectively,

$$A(j, i) = \frac{1}{s(j) + \gamma(i)},$$

$$b(j) = \frac{1}{s(j) \sigma v \Delta E} \left( \frac{q \mu_0 F S N_0}{\hat{I}(j)} - s(j) - \frac{1}{\tau_R} \right),$$

where  $\gamma(i) = \nu \exp\left(\frac{-E_i}{kT}\right)$ ,  $s(j) = \frac{1}{t_j}$  and  $\hat{I}(j) = \hat{I}(s_j)$ .

The DOS vector is then given by

$$g = A^{-1}b. \quad (12)$$

This expression constitutes the basis of the transient method that returns for  $\hat{I}(j)$  (i.e. the TPC data) a DOS distribution  $g(E)$  of localized states.

### 3. Experiment

#### 3.1. Preparation of sample

[15] A P-doped sample of a-Si:H was prepared by RF glow discharge decomposition of  $\text{SiH}_4$  with 3 vppm  $\text{PH}_3$ . Coplanar Al electrodes of 0.5 mm gap and 5 mm width were deposited on top of the film of 1  $\mu\text{m}$  thickness, and the voltage applied across the gap was 400 V (i.e. an electric field of 8000  $\text{Vcm}^{-1}$ ). The light source employed was a Laser Science VSL337  $\text{N}_2$ -pumped 5 ns pulse dye laser, 640 nm, producing pulsed carrier densities of up to  $10^{20} \text{ cm}^{-3}$ , varied by means of neutral density filters. Single shots or low frequency ( $< 1\text{Hz}$ ) laser pulses were used to allow complete carrier relaxation. The TPC signal was amplified where necessary, and measured using a PC-controlled Tektronix TDS380 oscilloscope as a transient recorder. A temperature range from 120–400 K was covered using a cryostat operating at a chamber pressure of typically  $10^{-4}$  Torr. The dark Fermi level was estimated from the dark conductivity measurement to be 0.5 eV below the conduction band mobility edge.

#### 3.2. Results

In the following, the free carriers lifetime  $\tau_R$  and the energy profile of the DOS  $g(E)$  are determined from an experimental TPC data. TPC are then generated by numerical simulation, using these  $\tau_R$  and DOS, and compared to the experimental ones.

Fig. 5 shows a set of five TPC decays for the P-doped a-Si:H sample at 150, 200, 250, 290 and 310 K measured with an excitation density of  $N_0 = 10^{16} \text{ cm}^{-3}$ .

To valid the proposed method for the experimental case, we determinate  $\tau_R$  and exact DOS  $g(E)$  from the experimental TPC data of Fig. 5. We then simulate TPC using these  $\tau_R$  and DOS  $g(E)$  in order to reproduce the experimental ones. Using Eq. (7) for measured TPC decays at 200, 250 and 310K of Fig. 5, we find respectively the following values of  $\tau_R$ :  $1.2933 \times 10^{-6}$  s,  $9.7965 \times 10^{-7}$  s and  $8.552 \times 10^{-7}$  s. And by inserting these values of  $\tau_R$  into Eq. (10) for each case (200, 250 and 310K), we determine the energy profile of the DOS  $g(E)$  after calculating the corresponding  $\hat{I}(s)$  (Eq. (5)).

Fig. 6 shows the portion DOS  $g(E)$ , calculated by the inversion of Eq. (10), in the P-doped sample of Fig. 5 for the temperatures 200, 250 and 310K. The solid line is the DOS model obtained by fitting of the experimental DOS to the DOS expression:

$$g(E) = g(E_c) \exp\left(\frac{E}{kT_{c1}}\right) \left[ 1 - \frac{1}{1 + \exp\left(\frac{E - E_d}{kT_{c2}}\right)} \right] + g_g \exp\left[-\left(\frac{E - E_g}{E_w}\right)^2\right]. \quad (13)$$

Equation (13) indicates that the DOS model presents two exponential distributions parts on which a Gaussian distribution has been superimposed. One exponential distribution above  $E_d$  with high characteristic temperature  $T_{c1}$  and the other below  $E_d$  with low characteristic temperature  $T_c = \frac{T_{c1}T_{c2}}{T_{c1} + T_{c2}}$ . Least squares fitting gives  $g(E_c) = 3.2279 \times 10^{21} \text{ cm}^{-3} \text{ eV}^{-1}$ ,  $E_d = 0.12417 \text{ eV}$  below  $E_c$ ,  $T_{c1} = 1321.3 \text{ K}$  and  $T_{c2} = 211.49 \text{ K}$ , resulting in  $T_c \approx 182.3 \text{ K}$ . For the Gaussian distribution,  $g_g = 3.1292 \times 10^{15} \text{ cm}^{-3} \text{ eV}^{-1}$ ,  $E_g = 0.36888 \text{ eV}$  below  $E_c$  and  $E_w = 29.685 \text{ meV}$ . The result is a well-defined steep exponential conduction band tail of characteristic temperature  $T_c$  with a slight deviation towards  $E_c$  at the top to which is added a Gaussian distribution of energy width  $E_w$  and whose the peak, of value  $g_g$ , is positioned at  $E_g$  below the mobility edge  $E_c$ . The doping effect on the tail shape is remarkable, the DOS

with energies around the donor (P) band peak at a certain level  $E_d$  between 0.1eV and 0.2eV below  $E_c$  [16] is found to increase with doping. The DOS is then, a broad distribution above  $E_d$ , a narrow tail below it and a deeper Gaussian distribution, so that the DOS profile can be fitted with the DOS model of Eq. (13).

The parameters used to perform  $\tau_R$  and the DOS  $g(E)$  are the following:

$$\mu_0 = 10 \text{ cm}^2 \text{ s}^{-1} \text{ V}^{-1}, C_n = \sigma \nu = 2 \times 10^{-8} \text{ cm}^3 \text{ s}^{-1} \text{ and } \nu = 10^{12} \text{ s}^{-1}.$$

Fig. 7 shows the computed TPC decays (solid lines) for the P-doped sample at temperatures 200, 250 and 310K using the DOS model of Fig. 6. The corresponding experimental TPC decays of Fig. 5 are also presented (symbols). It turns out that, the modelled TPC curves line up quite rigorously with the experimental ones.

## 4. Discussion

### 4.1. Temperature effect

Limitations of the method are essentially the effect of low temperatures of TPC measurement on  $\tau_R$  when the recombination phenomenon is not observed at short times. Fig.

9 shows the TPC,  $n(t)$ , computed at 150K between initial time  $t_i = \frac{1}{\nu}$  and various values of

final time  $t_f = \frac{1}{\nu} \exp\left(\frac{E_c - E}{kT}\right)$  for the proposed exponential plus Gaussian DOS model of Fig.

8 with  $\tau_R = 10^{-8} \text{ s}$ . The chosen  $t_f$  are, respectively, 1,  $10^2$  and  $10^4 \text{ s}$ . The corresponding calculated  $\tau_R$  using Eq. (7) are, respectively,  $2.9693 \times 10^{-9}$ ,  $9.8854 \times 10^{-8}$  and  $7.3038 \times 10^{-7} \text{ s}$ .

It can be seen here that the proposed method does not recover the introduced  $\tau_R$ . We can retrieve the 'exact' value of the pre-proposed  $\tau_R$  for low temperatures, provided to take extremely long times, which is not feasible experimentally. In conclusion we can say that the method is influenced by the temperature, it is valid only when the phenomenon of

1  
2 recombination is observable, that is to say in the case of high temperatures. Higher  
3  
4 temperature is better, as it shifts the recombination feature to shorter times, into the accessible  
5  
6 time-region. Therefore, at low temperatures there is a little evidence of the effect of  
7  
8 recombination on TPC over the experimental timescale.  
9

#### 10 11 4.2. Truncated data

12  
13 Fig. 10 shows the TPC,  $n(t)$  (solid line), computed at 350K between initial time  $t_i = 1$  ps  
14  
15 and final time  $t_f = 1$  s for the proposed exponential plus Gaussian DOS model of Fig. 2a with  
16  
17  $\tau_R = 10^{-8}$  s and the truncated  $n(t)$  (symbol o) at time 10 ns after  $t_i$ , i.e. 10 ns is the new  
18  
19 starting time  $t_i$ . For the full data  $n(t)$ ,  $\tau_R$  was already been calculated (section 2.1), it is  
20  
21 worth  $8.7256 \times 10^{-9}$  s and for the truncated one,  $\tau_R$  is equal to  $8.5912 \times 10^{-9}$  s, it was  
22  
23 calculated in the same way as in the case of complete data (Eq. 7). Fig. 11 shows the same full  
24  
25 TPC,  $n(t)$  (solid line) as of Fig. 10 and the truncated  $n(t)$  (symbol o) at time  $100 \mu\text{s}$  before  
26  
27  $t_f$ , i.e.  $100 \mu\text{s}$  is the new final time  $t_f$ . For the truncated one,  $\tau_R$  is equal to  $8.7217 \times 10^{-9}$  s.  
28  
29 As we see the estimation of  $\tau_R$  is not influenced by the missing of short or long time data.  
30  
31 This implies that there must be some influence of recombination at short times, long before  
32  
33 the 'final' recombination decay which we normally expect (and see) at long times.  
34  
35  
36  
37  
38  
39  
40

#### 41 42 4.3. Noisy data

43  
44 Accuracy of measuring  $\tau_R$  has been already investigated by application to simulated  
45  
46 (perfect) data, but how good is it when used on real (imperfect) data, subject to noise? To do  
47  
48 this, we simulate TPC,  $n(t)$ , for given DOS model and  $\tau_R$ , and add Gaussian noise whose  
49  
50 amplitude is a constant fraction of  $n(t)$ . Random noise is approximately Gaussian of similar  
51  
52 amplitude over whole time range. Noise was introduced by multiplying each point of  $n(t)$  by  
53  
54 a random number from a Gaussian distribution whose mean value is 1. The standard deviation  
55  
56 of the distribution was varied between 10% and 40%.  
57  
58  
59  
60

1  
2 Fig. 12 shows the simulated (smoothed) TPC,  $n(t)$  (solid line), of Fig. 2b and the noisy  
3  
4  $n(t)$  (symbol o) when noise level is equal to 10%. Eq. (7) gives  $\tau_R = 8.7256 \times 10^{-9}$  s for  
5  
6 simulated  $n(t)$  and  $9.0484 \times 10^{-9}$  s for noisy  $n(t)$  when the used  $\tau_R$  in the simulation of  $n(t)$   
7  
8 is  $10^{-8}$  s. It can be seen that the estimation of  $\tau_R$  is not influenced by noise.  
9

10  
11  
12 Fig. 13 shows the deviation  $\frac{\text{smoothed data} - \text{noisy data}}{\text{smoothed data}}$  versus time in the case of 10%  
13  
14 noise. As we see Gaussian noise is approximately uniform over entire time range.  
15  
16  
17

18  
19 Fig. 14 shows estimated  $\tau_R$  versus noise level, this last varying between 10% and 40%.  
20  
21  $\tau_R$  remains practically constant, and equal to  $10^{-8}$  s, over whole noise level range. The  
22  
23 method is 'noise tolerant', it is capable of returning optimal resolution for a given set of noisy  
24  
25 data even at quite high input noise levels.  
26  
27  
28  
29  
30  
31  
32  
33  
34  
35  
36  
37  
38  
39  
40  
41  
42  
43  
44  
45  
46  
47  
48  
49  
50  
51  
52  
53  
54  
55  
56  
57  
58  
59  
60

## 5. Conclusion

We have proposed a new method for determining the free carriers lifetime  $\tau_R$  and the density of localized states DOS in amorphous semiconductors from the transient photocurrent TPC data. This technique involves Laplace transform of TPC data, it is a simple analysis of the solution of the basic linearized multiple trapping equations for free and trapped electrons. It has been tested by applying it to simulated and experimental TPC data measured on a typical disordered semiconductor, the hydrogenated amorphous silicon (a-Si:H). An introduced  $\tau_R$  in the computing of the TPC using an arbitrarily proposed DOS model is recovered with high accuracy. For the experimental case, the estimated  $\tau_R$  and the determination of the exact DOS from the experimental TPC data allow to reconstruct accurately this last. Limitations of the technique are essentially the effect of low temperatures of TPC measurement on  $\tau_R$  when the recombination phenomenon is not observed at short times. On the other hand, the determination of  $\tau_R$  is not at all influenced by the missing of short or long time data and the noisy data.

**Acknowledgements**

The authors thank Amorphous Semiconductors group at Dundee University for the measurement facilities. The Algerian Ministry of Higher Education and Research is acknowledged for his financial support.

For Peer Review Only



## References

- [1] R. H. Bube, Photoelectric Properties of Semiconductors, Cambridge Univ. Press, Cambridge, 1992.
- [2] J. Orenstein, M.A. Kastner, V. Vaninov, Philos. Mag. B 46 (1982) 23.
- [3] G. Seynhaeve, G.J. Adriaenssens, H. Michiel, Solid State Commun. 56 (1985) 323.
- [4] G.J. Adriaenssens, S. D. Baranovskii, W. Fuhs, J. Jansen, Ö. Öktü, Phys. Rev. B 51 (1995) 9661.
- [5] T. Nagase, H. Naito, J. Non-Cryst. Solids 227-230 (1998) 824.
- [6] R. R. Koropecki, J. A. Schmidt, R. Arce, J. Appl. Phys. 91 (2002) 8965.
- [7] H. Naito, J. Ding, M. Okuda, Appl. Phys. Lett. 64 (1994) 1830.
- [8] H. Naito, M. Okuda, J. Appl. Phys. 77 (1995) 3541.
- [9] H. Naito, T. Nagase, T. Ishii, M. Okuda, T. Kawaguchi, S. Maruno, J. Non-Cryst. Solids 198-200 (1996) 363.
- [10] N. Ogawa, T. Nagase, H. Naito, J. Non-Cryst. Solids 266-269 (2000) 367.
- [11] M.R. Spiegel, Schaum's Outline of Theory and Problems of Laplace transforms (McGraw-Hill 1965).
- [12] T. Nagase, K. Kishimoto, H. Naito, J. Appl. Phys. 86 (1999) 5026.
- [13] A. N. Tikhonov, A. V. Goncharsky, V. V. Stepanov, A. G. Yagola, Numerical Methods for the Solution of ill-Posed Problems, Kluwer, Dordrecht, 1995.
- [14] J. Weese, Comput. Phys. Commun. 69 (1992) 99.
- [15] A Merazga, A F Meftah, A M Meftah, C Main and S Reynolds, J. Phys.: Condens. Matter 13 (2001) 10969
- [16] R. A. Street, Hydrogenated amorphous silicon, Cambridge University Press (1991).

## Figure captions

Fig. 1. (a) - Exponential DOS model with  $g(E_c) = 10^{21} \text{ cm}^{-3} \text{ eV}^{-1}$  and characteristic temperature  $T_c = 400 \text{ K}$ .

(b) - Simulated TPC,  $n(t)$ , at 300 K using DOS of (a) for different  $\tau_R$  values.

Fig. 2. (a) - Exponential plus Gaussian distribution of states with  $g(E_c) = 10^{21} \text{ cm}^{-3} \text{ eV}^{-1}$ ,  $T_c = 400 \text{ K}$ ,  $g_g = 10^{19} \text{ cm}^{-3} \text{ eV}^{-1}$ ,  $E_g = -0.35 \text{ eV}$  and  $E_w = 40 \text{ meV}$ .

(b) - Simulated TPC,  $n(t)$ , at 350 K using DOS of (a) for  $\tau_R = 10^{-8} \text{ s}$ .

Fig. 3. (a) -  $n(t)$  (symbol o) of fig 1 (b) for  $\tau_R = 10^{-6} \text{ s}$  and  $\tau_R (s^{-1})$  (solid line) for corresponding  $\hat{n}(s)$ . For clarity, the curve  $n(t)$  is multiplied by the factor  $10^{-20}$ .

(b) -  $n(t)$  (symbol o) of fig 1 (b) for  $\tau_R = 10^{-7} \text{ s}$  and  $\tau_R (s^{-1})$  (solid line) for corresponding  $\hat{n}(s)$ . For clarity, the curve  $n(t)$  is multiplied by the factor  $10^{-21}$ .

(c) -  $n(t)$  (symbol o) of fig 1 (b) for  $\tau_R = 10^{-8} \text{ s}$  and  $\tau_R (s^{-1})$  (solid line) for corresponding  $\hat{n}(s)$ . For clarity, the curve  $n(t)$  is multiplied by the factor  $10^{-22}$ .

Fig. 4 -  $n(t)$  (symbol o) of fig 2 (b) and  $\tau_R (s^{-1})$  (solid line) for corresponding  $\hat{n}(s)$ . For clarity, the curve  $n(t)$  is multiplied by the factor  $10^{-21}$ .

Fig. 5 - Measured TPC decays for the P-doped a-Si:H sample at five different temperatures (150, 200, 250, 290 and 310 K) with an excitation density of  $N_0 = 10^{16} \text{ cm}^{-3}$ .

Fig. 6 - Experimental DOS  $g(E)$  in the P-doped sample of Fig. 5 for the temperatures 200, 250 and 310 K (symbols). The solid line is the DOS model obtained by fitting of the experimental DOS with Eq. (13).

Fig. 7 - Simulated TPC decays (full curves) for the P-doped sample at temperatures 200, 250 and 310 K using the DOS model of Fig.7, showing good reconstruction of the corresponding experimental ones (symbols). The curves are offset vertically for clarity.

1  
2 Fig. 8 - Exponential plus Gaussian distribution of states for various values of final time  $t_f$ ,

3  
4 with  $g(E_c) = 10^{21} \text{ cm}^{-3} \text{ eV}^{-1}$ ,  $T_c = 400 \text{ K}$ ,  $g_g = 10^{19} \text{ cm}^{-3} \text{ eV}^{-1}$ ,  $E_g = -0.3 \text{ eV}$  and

5  
6  
7  $E_w = 40 \text{ meV}$ . The curves are offset vertically for clarity.

8  
9  
10 Fig. 9 - Simulated TPC,  $n(t)$ , at 150 K using corresponding DOS of Fig. 8 for  $\tau_R = 10^{-8} \text{ s}$ .

11  
12 The curves are offset vertically for clarity.

13  
14 Fig. 10 - Full TPC,  $n(t)$  (solid line), of Fig. 2b and truncated  $n(t)$  (symbol o) at time 10 ns.

15  
16 Fig. 11 - Full TPC,  $n(t)$  (solid line), of Fig. 11 and truncated  $n(t)$  (symbol o) at time 100  $\mu\text{s}$ .

17  
18 Fig. 12 - Smoothed TPC,  $n(t)$  (solid line), of Fig. 2b and noisy  $n(t)$  (symbol o) (10% noise).

19  
20 Fig. 13 - Deviation  $\frac{\text{smoothed data} - \text{noisy data}}{\text{smoothed data}}$  versus time (10% noise).

21  
22  
23  
24  
25  
26  
27 Fig. 14 -  $\tau_R$  versus noise level.

Figures

Figure 1

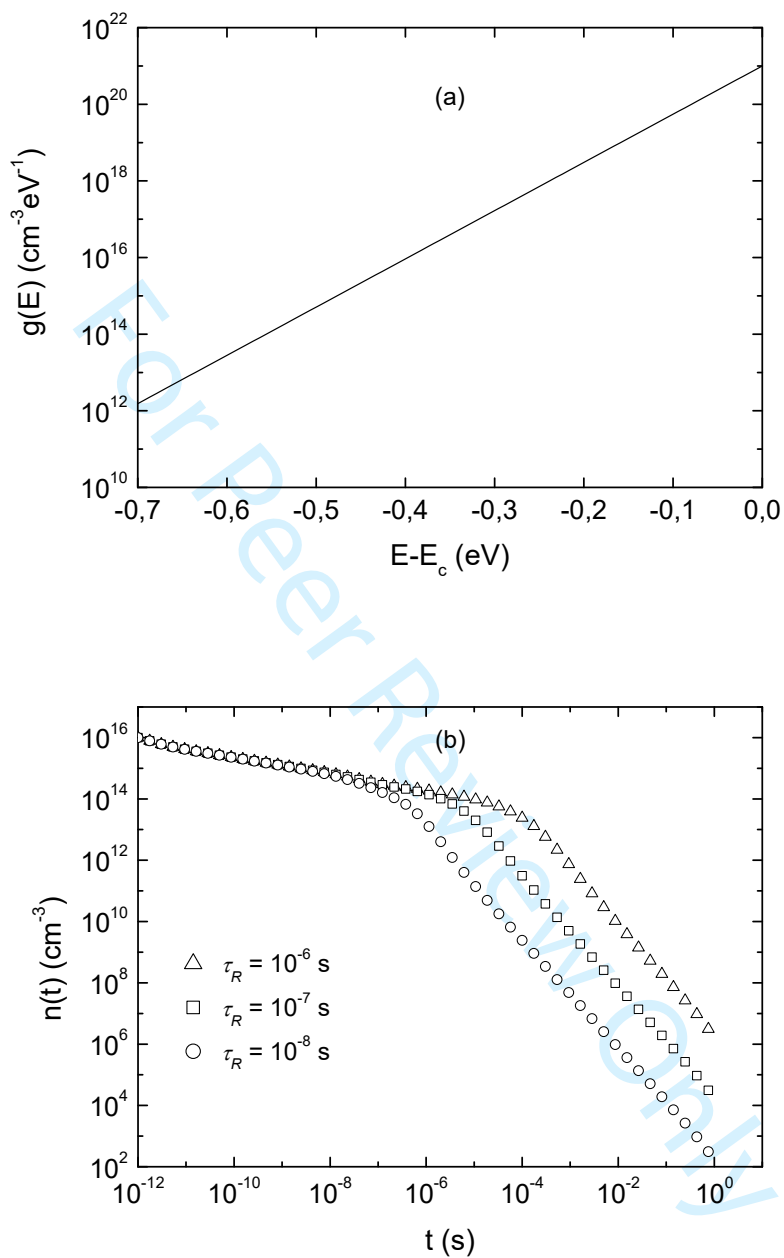


Figure 2

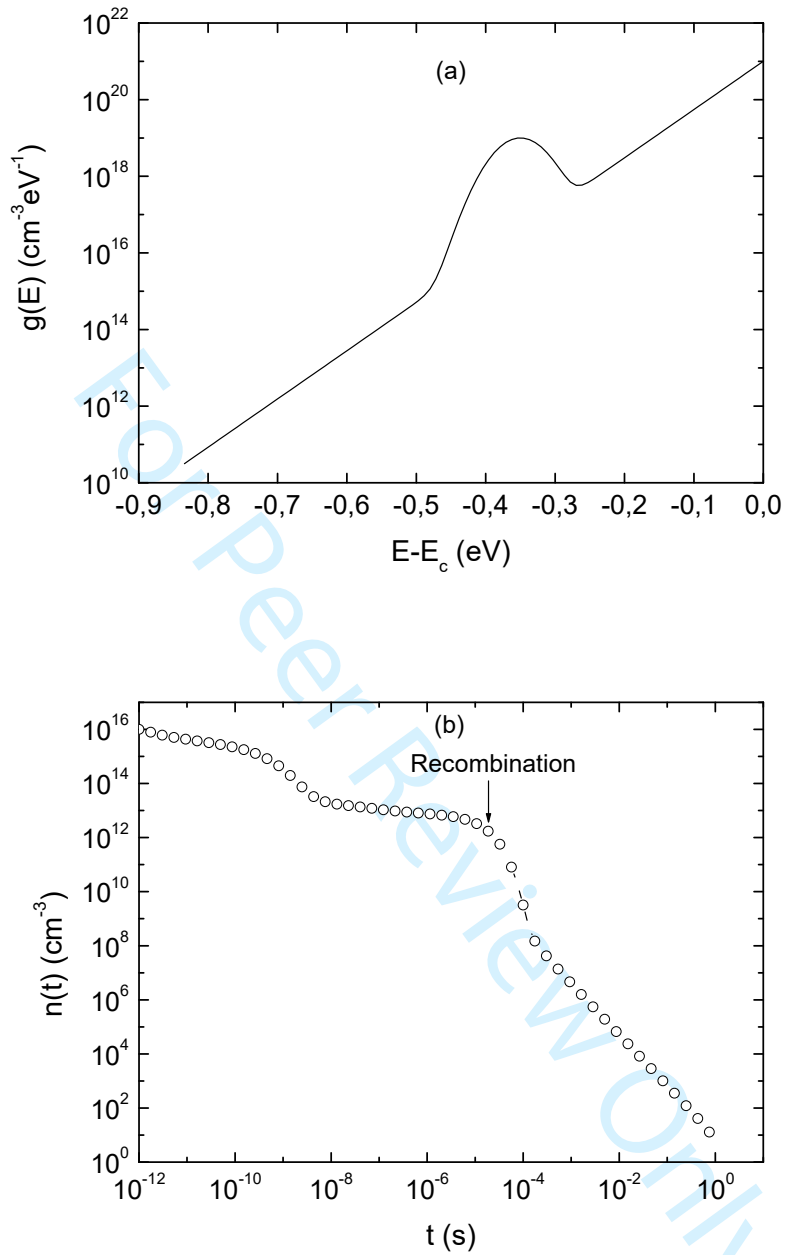
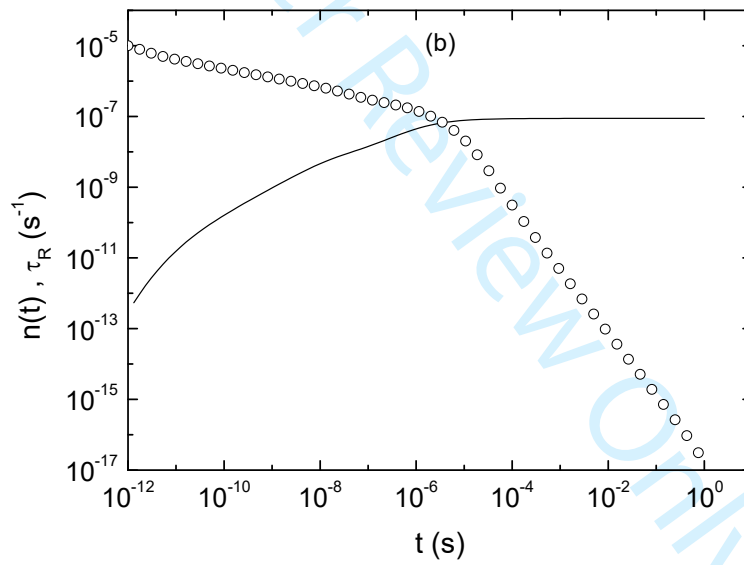
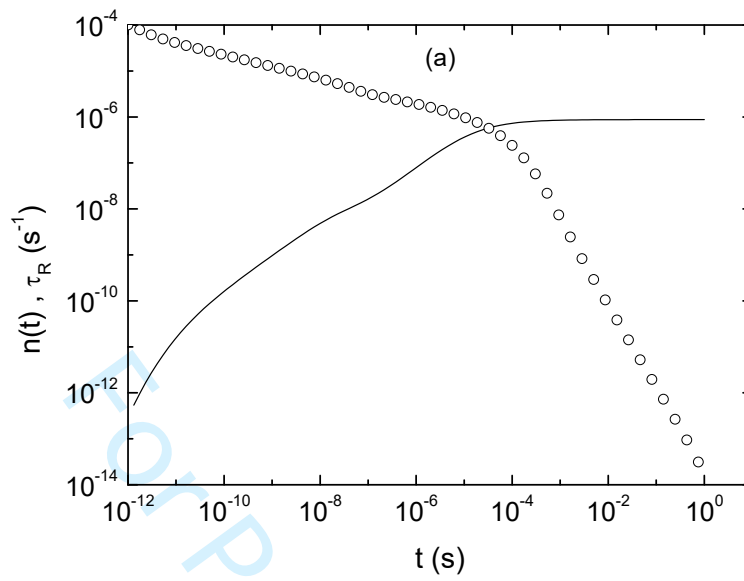


Figure 3



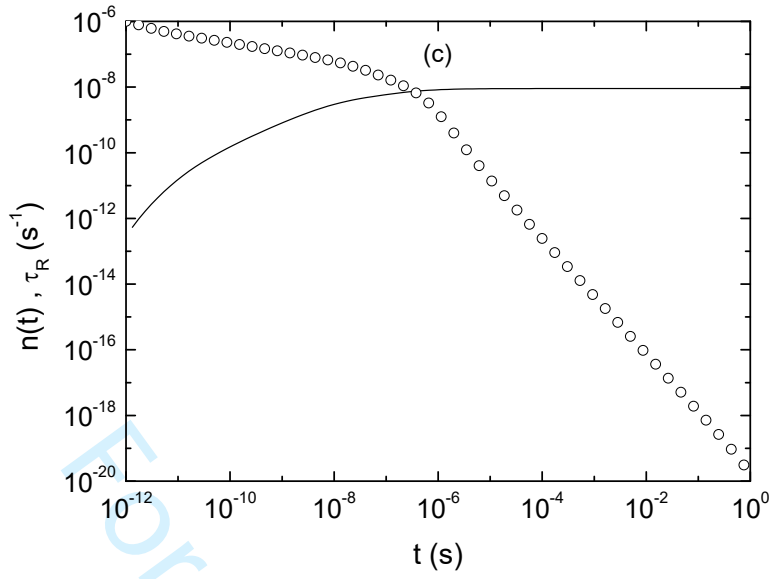


Figure 4

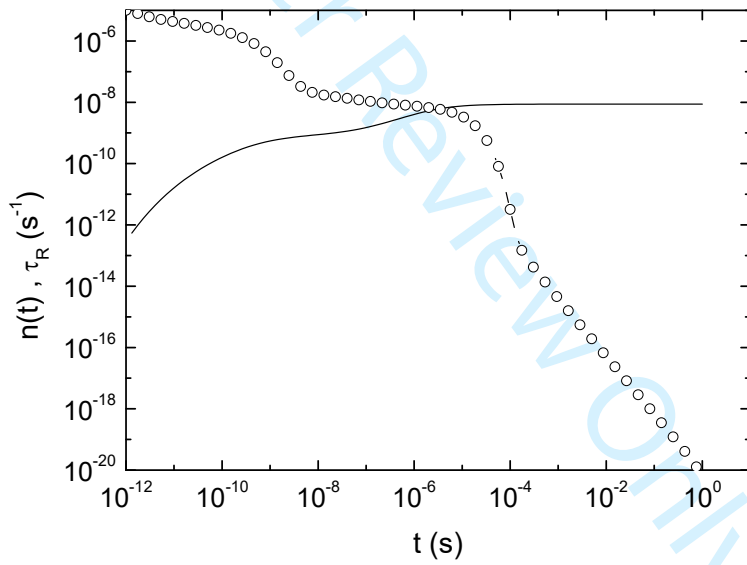


Figure 5

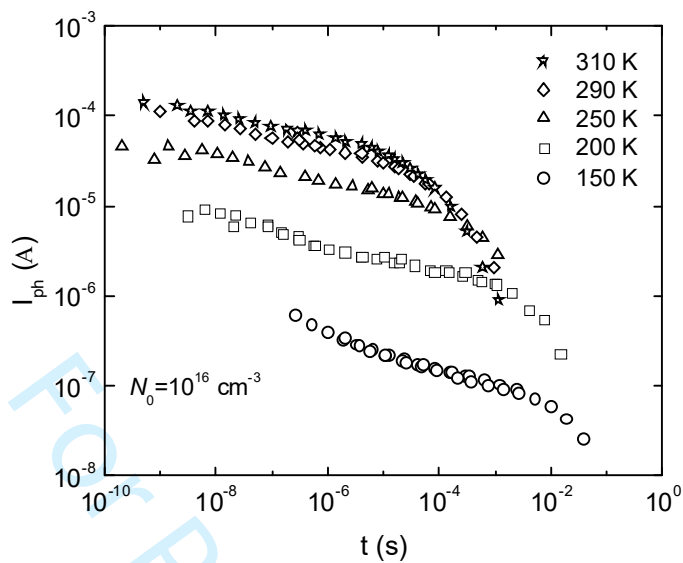


Figure 6

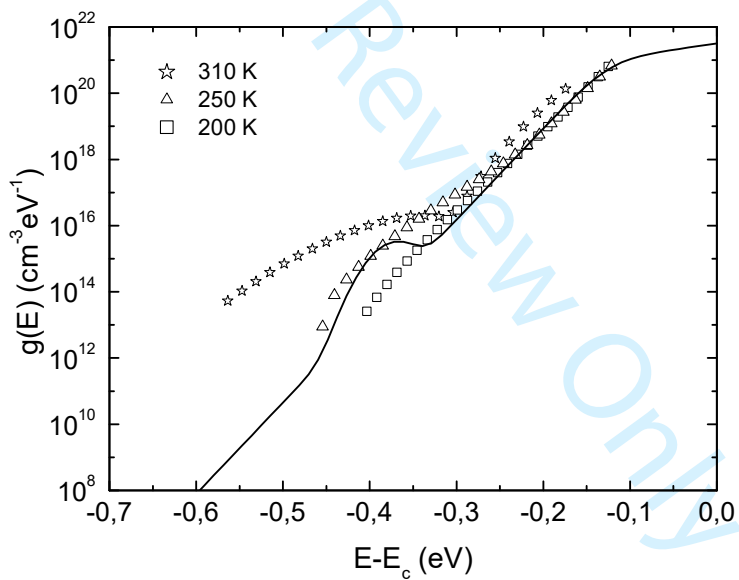




Figure 7

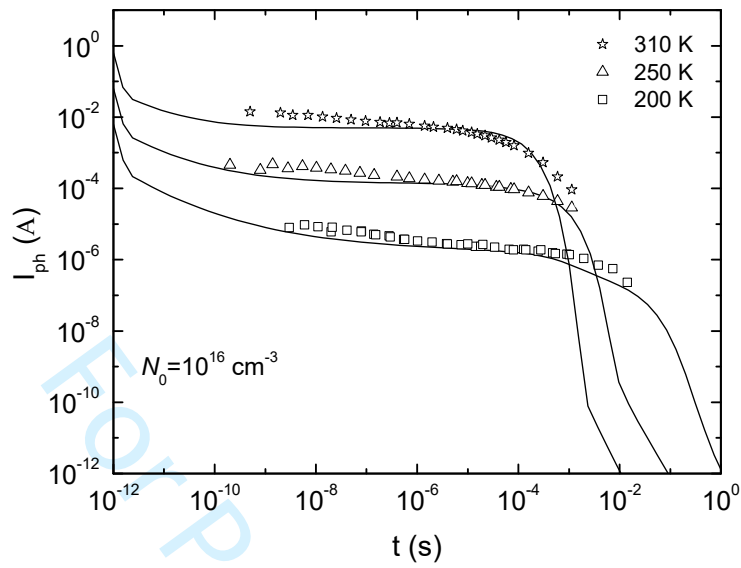


Figure 8

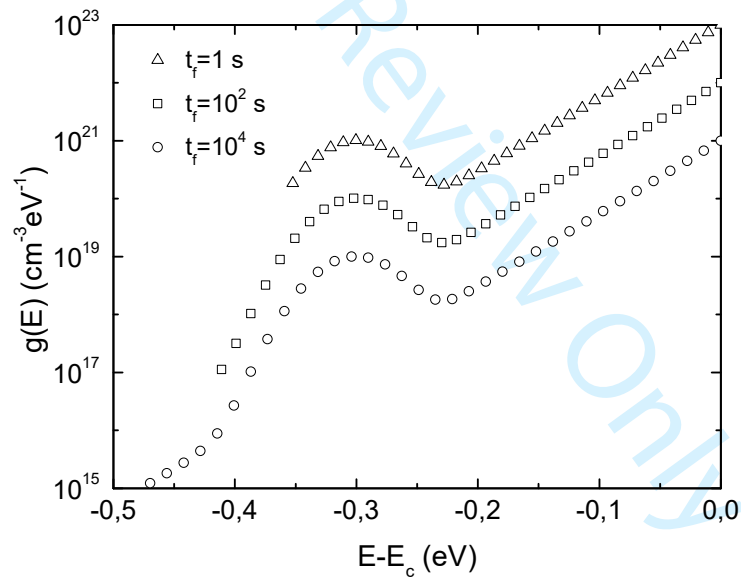


Figure 9

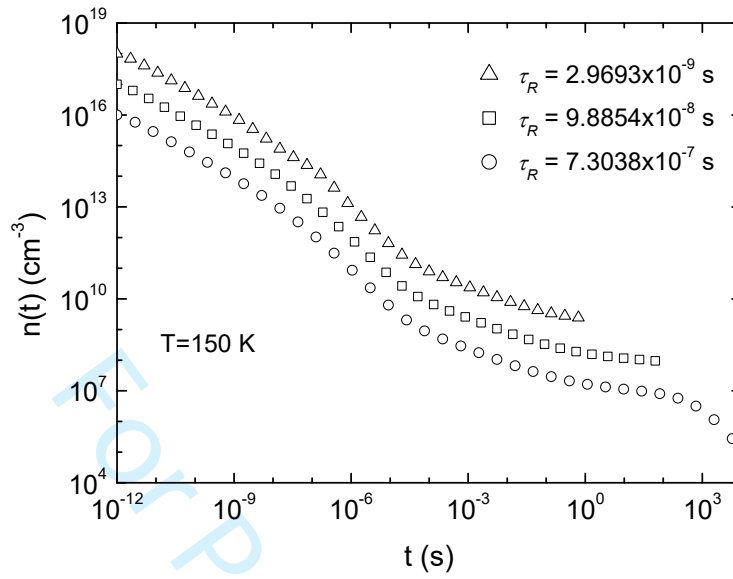


Figure 10

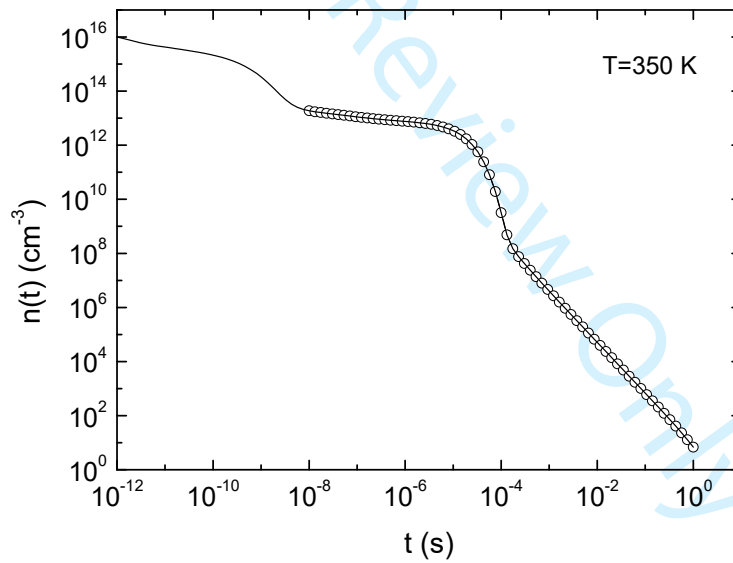


Figure 11

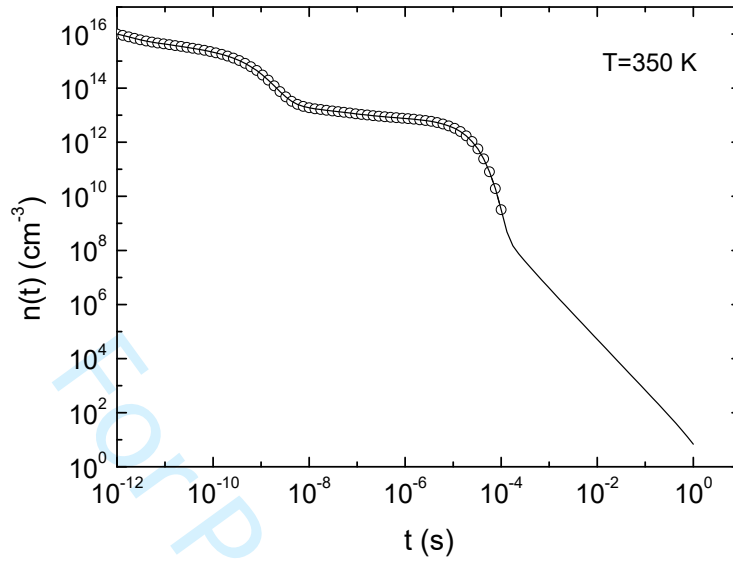


Figure 12

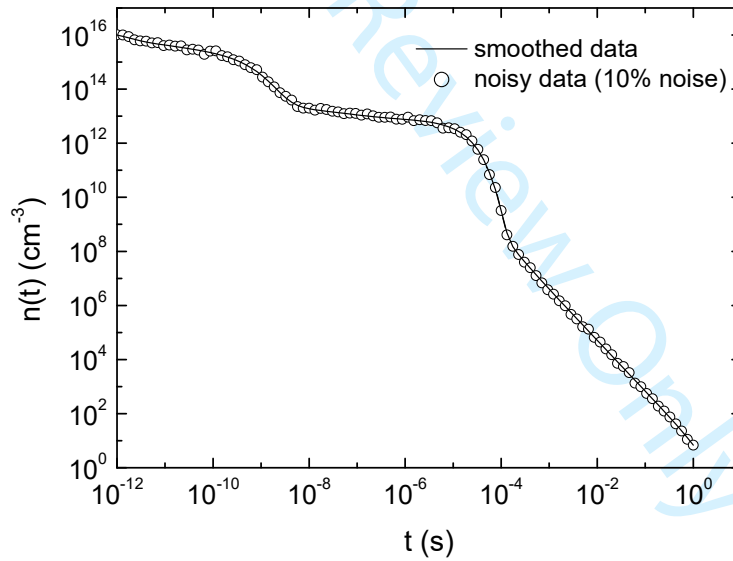


Figure 13

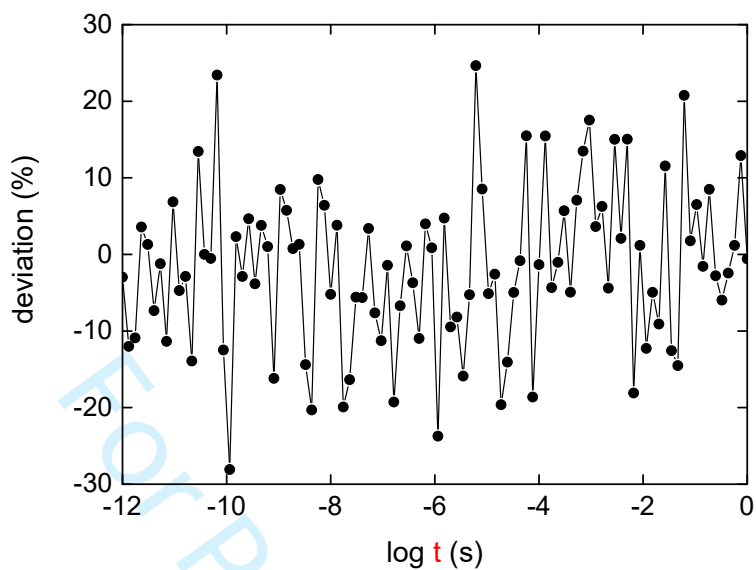
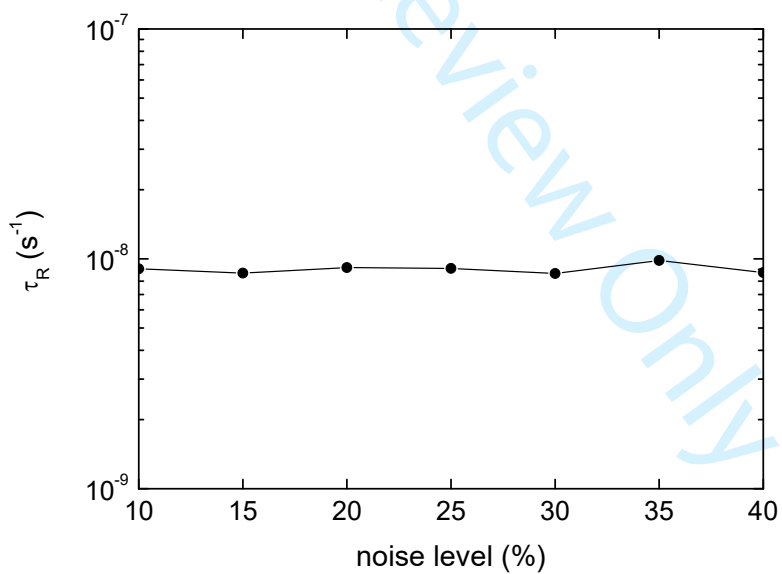
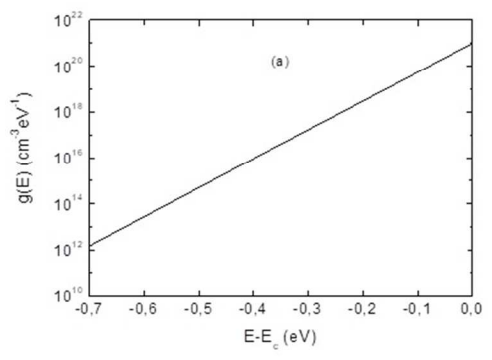


Figure 14

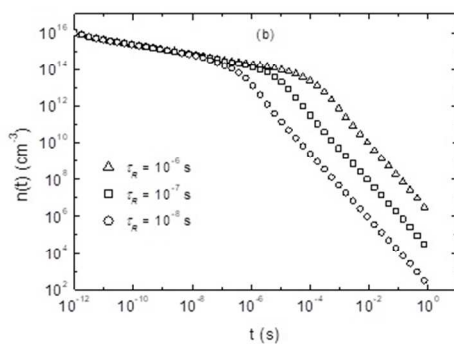


1  
2  
3  
4  
5  
6  
7  
8  
9  
10  
11  
12  
13  
14  
15  
16  
17  
18  
19  
20  
21  
22  
23  
24  
25  
26  
27  
28  
29  
30  
31  
32  
33  
34  
35  
36  
37  
38  
39  
40  
41  
42  
43  
44  
45  
46  
47  
48  
49  
50  
51  
52  
53  
54  
55  
56  
57  
58  
59  
60



216x121mm (96 x 96 DPI)

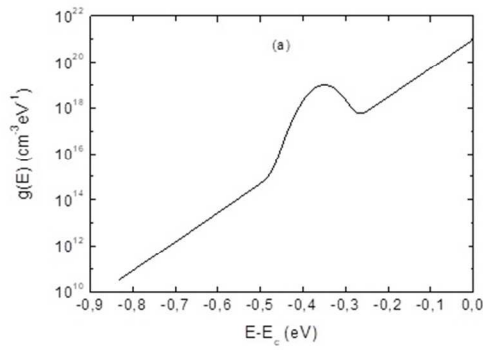
Review Only



216x121mm (96 x 96 DPI)

Review Only

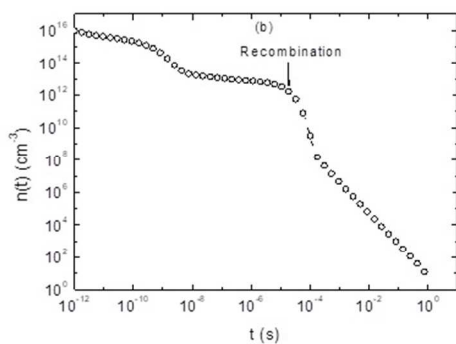
1  
2  
3  
4  
5  
6  
7  
8  
9  
10  
11  
12  
13  
14  
15  
16  
17  
18  
19  
20  
21  
22  
23  
24  
25  
26  
27  
28  
29  
30  
31  
32  
33  
34  
35  
36  
37  
38  
39  
40  
41  
42  
43  
44  
45  
46  
47  
48  
49  
50  
51  
52  
53  
54  
55  
56  
57  
58  
59  
60



216x121mm (96 x 96 DPI)

Review Only

1  
2  
3  
4  
5  
6  
7  
8  
9  
10  
11  
12  
13  
14  
15  
16  
17  
18  
19  
20  
21  
22  
23  
24  
25  
26  
27  
28  
29  
30  
31  
32  
33  
34  
35  
36  
37  
38  
39  
40  
41  
42  
43  
44  
45  
46  
47  
48  
49  
50  
51  
52  
53  
54  
55  
56  
57  
58  
59  
60

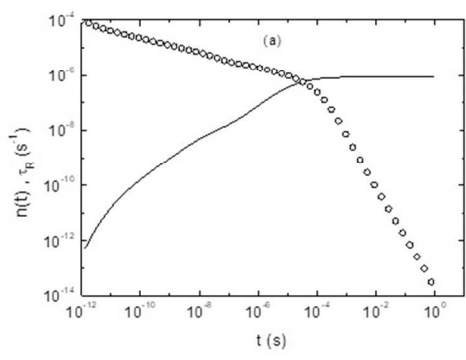


216x121mm (96 x 96 DPI)

Review Only



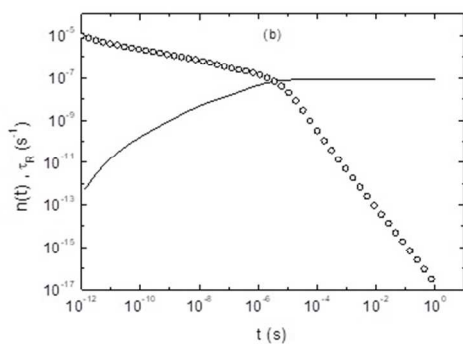
1  
2  
3  
4  
5  
6  
7  
8  
9  
10  
11  
12  
13  
14  
15  
16  
17  
18  
19  
20  
21  
22  
23  
24  
25  
26  
27  
28  
29  
30  
31  
32  
33  
34  
35  
36  
37  
38  
39  
40  
41  
42  
43  
44  
45  
46  
47  
48  
49  
50  
51  
52  
53  
54  
55  
56  
57  
58  
59  
60



216x121mm (96 x 96 DPI)

Review Only

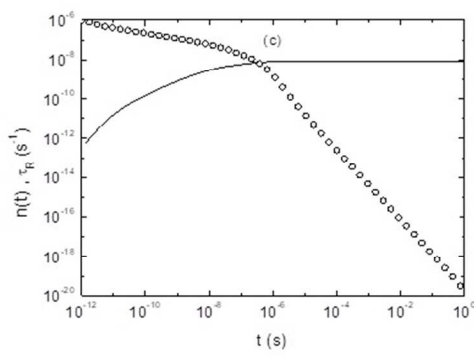
1  
2  
3  
4  
5  
6  
7  
8  
9  
10  
11  
12  
13  
14  
15  
16  
17  
18  
19  
20  
21  
22  
23  
24  
25  
26  
27  
28  
29  
30  
31  
32  
33  
34  
35  
36  
37  
38  
39  
40  
41  
42  
43  
44  
45  
46  
47  
48  
49  
50  
51  
52  
53  
54  
55  
56  
57  
58  
59  
60



216x121mm (96 x 96 DPI)

Review Only

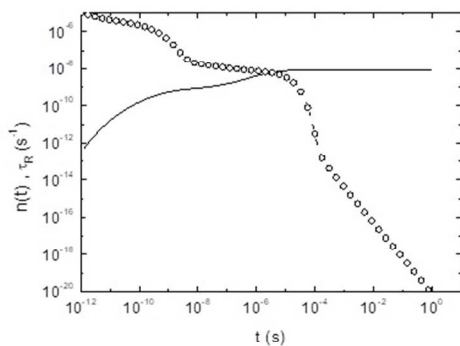
1  
2  
3  
4  
5  
6  
7  
8  
9  
10  
11  
12  
13  
14  
15  
16  
17  
18  
19  
20  
21  
22  
23  
24  
25  
26  
27  
28  
29  
30  
31  
32  
33  
34  
35  
36  
37  
38  
39  
40  
41  
42  
43  
44  
45  
46  
47  
48  
49  
50  
51  
52  
53  
54  
55  
56  
57  
58  
59  
60



216x121mm (96 x 96 DPI)

Review Only

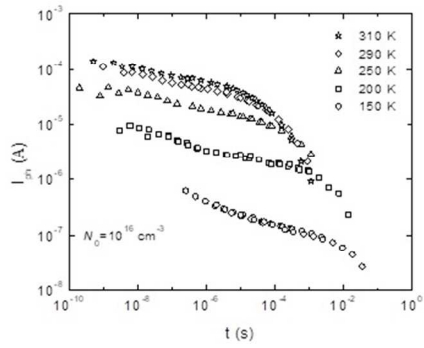
1  
2  
3  
4  
5  
6  
7  
8  
9  
10  
11  
12  
13  
14  
15  
16  
17  
18  
19  
20  
21  
22  
23  
24  
25  
26  
27  
28  
29  
30  
31  
32  
33  
34  
35  
36  
37  
38  
39  
40  
41  
42  
43  
44  
45  
46  
47  
48  
49  
50  
51  
52  
53  
54  
55  
56  
57  
58  
59  
60



216x121mm (96 x 96 DPI)

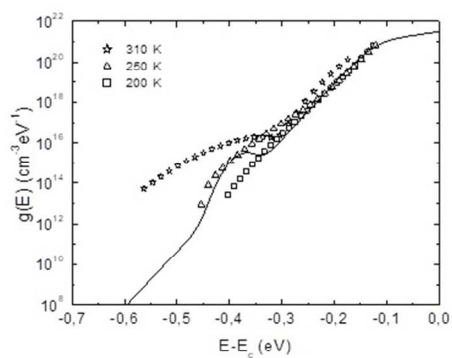
Review Only

1  
2  
3  
4  
5  
6  
7  
8  
9  
10  
11  
12  
13  
14  
15  
16  
17  
18  
19  
20  
21  
22  
23  
24  
25  
26  
27  
28  
29  
30  
31  
32  
33  
34  
35  
36  
37  
38  
39  
40  
41  
42  
43  
44  
45  
46  
47  
48  
49  
50  
51  
52  
53  
54  
55  
56  
57  
58  
59  
60



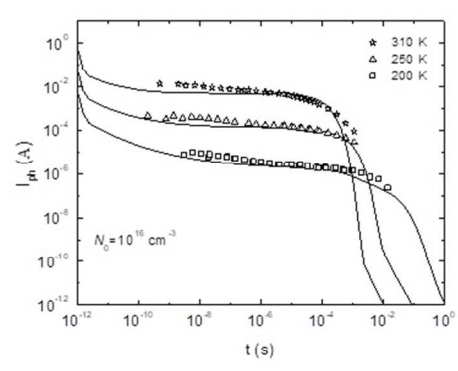
216x121mm (96 x 96 DPI)

Review Only



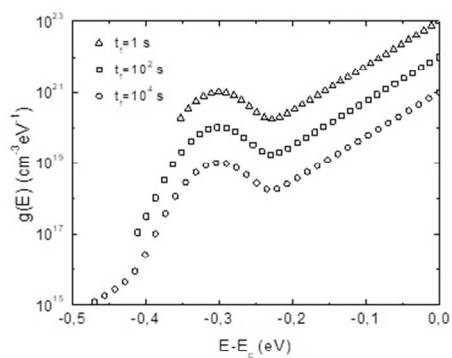
216x121mm (96 x 96 DPI)

1  
2  
3  
4  
5  
6  
7  
8  
9  
10  
11  
12  
13  
14  
15  
16  
17  
18  
19  
20  
21  
22  
23  
24  
25  
26  
27  
28  
29  
30  
31  
32  
33  
34  
35  
36  
37  
38  
39  
40  
41  
42  
43  
44  
45  
46  
47  
48  
49  
50  
51  
52  
53  
54  
55  
56  
57  
58  
59  
60



216x121mm (96 x 96 DPI)

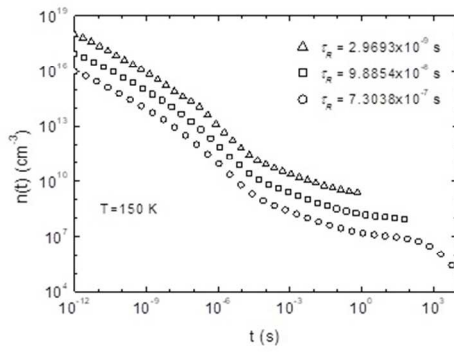
Review Only



216x121mm (96 x 96 DPI)



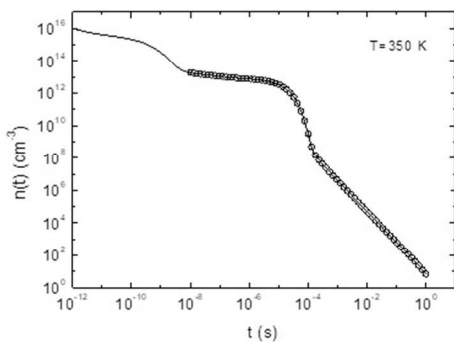
1  
2  
3  
4  
5  
6  
7  
8  
9  
10  
11  
12  
13  
14  
15  
16  
17  
18  
19  
20  
21  
22  
23  
24  
25  
26  
27  
28  
29  
30  
31  
32  
33  
34  
35  
36  
37  
38  
39  
40  
41  
42  
43  
44  
45  
46  
47  
48  
49  
50  
51  
52  
53  
54  
55  
56  
57  
58  
59  
60



216x121mm (96 x 96 DPI)

Review Only

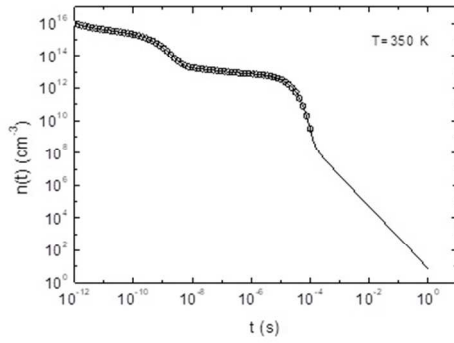
1  
2  
3  
4  
5  
6  
7  
8  
9  
10  
11  
12  
13  
14  
15  
16  
17  
18  
19  
20  
21  
22  
23  
24  
25  
26  
27  
28  
29  
30  
31  
32  
33  
34  
35  
36  
37  
38  
39  
40  
41  
42  
43  
44  
45  
46  
47  
48  
49  
50  
51  
52  
53  
54  
55  
56  
57  
58  
59  
60



216x121mm (96 x 96 DPI)

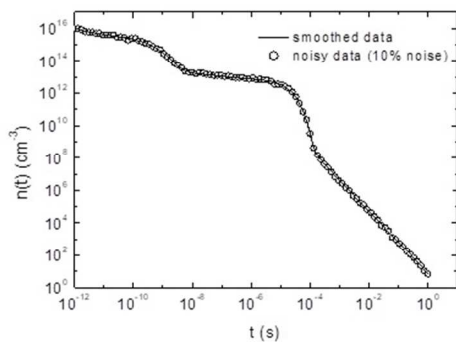
Review Only

1  
2  
3  
4  
5  
6  
7  
8  
9  
10  
11  
12  
13  
14  
15  
16  
17  
18  
19  
20  
21  
22  
23  
24  
25  
26  
27  
28  
29  
30  
31  
32  
33  
34  
35  
36  
37  
38  
39  
40  
41  
42  
43  
44  
45  
46  
47  
48  
49  
50  
51  
52  
53  
54  
55  
56  
57  
58  
59  
60



216x121mm (96 x 96 DPI)

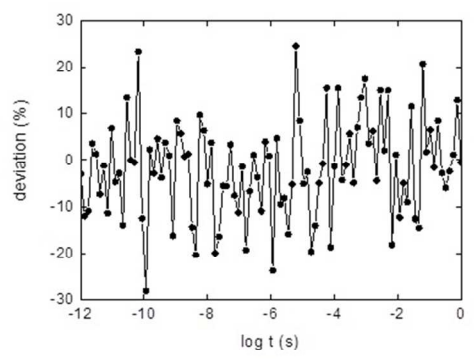
Review Only



216x121mm (96 x 96 DPI)

Review Only

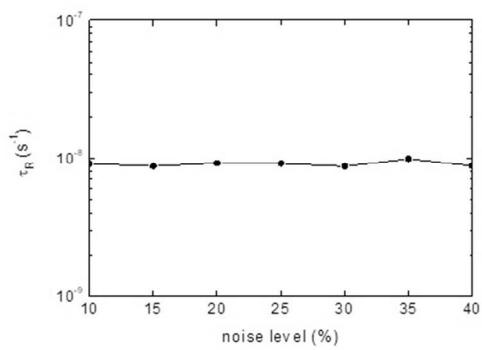
1  
2  
3  
4  
5  
6  
7  
8  
9  
10  
11  
12  
13  
14  
15  
16  
17  
18  
19  
20  
21  
22  
23  
24  
25  
26  
27  
28  
29  
30  
31  
32  
33  
34  
35  
36  
37  
38  
39  
40  
41  
42  
43  
44  
45  
46  
47  
48  
49  
50  
51  
52  
53  
54  
55  
56  
57  
58  
59  
60



216x121mm (96 x 96 DPI)

Review Only

1  
2  
3  
4  
5  
6  
7  
8  
9  
10  
11  
12  
13  
14  
15  
16  
17  
18  
19  
20  
21  
22  
23  
24  
25  
26  
27  
28  
29  
30  
31  
32  
33  
34  
35  
36  
37  
38  
39  
40  
41  
42  
43  
44  
45  
46  
47  
48  
49  
50  
51  
52  
53  
54  
55  
56  
57  
58  
59  
60



216x121mm (96 x 96 DPI)

Review Only

A new approach for determination of free carriers lifetime and density of localized states in  
disordered semiconductors

H. Belgacem<sup>a,\*</sup>, S. Reynolds<sup>b</sup>

<sup>a</sup> *Department of Physics, Faculty of Matter Science, University Hadj Lakhdar Batna 1, 5 avenue Chahid  
Boukhrouf, 05000 Batna, Algeria*

<sup>b</sup> *Physics Division, School of Engineering, Physics and Mathematics, University of Dundee, Dundee DD1 4HN,  
UK*

### Abstract

A new method for measuring the free carriers lifetime ( $\tau_R$ ) and the density of localized states (DOS) in amorphous semiconductors is described. The method is based on the analysis of transient photoconductivity (TPC) data using Laplace transform technique. This technique involves Laplace transform of TPC data, it is a simple analysis of the solution of the basic linearized multiple trapping equations for free and trapped electrons. It is demonstrated by application to simulated and experimental TPC data measured on a typical disordered semiconductor, the hydrogenated amorphous silicon (a-Si:H). An introduced  $\tau_R$  in the computing of the TPC using an arbitrarily proposed DOS model is recovered with high accuracy. For the experimental case, the determination of the exact DOS and the estimated  $\tau_R$  from the experimental TPC data allow to reconstruct accurately this last. The performance and limitations of the technique are studied by means of computer simulations. Limitations are essentially the low temperatures of measurement of TPC when the recombination phenomenon is not observed at short times.

*Keywords:* Transient Photocurrent; Recombination lifetime; DOS; Laplace transform

\* Corresponding author. Tel.: +213 6 62296115; fax: +213 33 319017.

*E-mail address:* [hocine.belgacem@univ-batna.dz](mailto:hocine.belgacem@univ-batna.dz) (H. Belgacem).

## 1. Introduction

Photodecay experiments have been used to measure the recombination lifetime of photogenerated carriers in semiconductors [1]. In amorphous semiconductors, the TPC decay experiments also enable us to determine the characteristic recombination time  $\tau_c$  from the transition point from the pre-transit photocurrent  $I_{ph}$  vary as  $t^{-(1-\alpha)}$  to the post-transit one vary as  $t^{-(1+\alpha)}$  in case of the monomolecular recombination process [2] and by assuming an exponential decreasing density of localized states  $g(E) = g(E_c) \exp\left(\frac{-E}{kT_c}\right)$ , where  $\alpha = \frac{T}{T_c}$  for  $T < T_c$  is the dispersion parameter. Transitions to the post-transit region occur at various times, increasing with increasing  $\tau_R$ . The  $\tau_c$  can be related to  $\tau_R$  by assuming the thermalization of photogenerated carriers into an exponential band tail of localized defects [2]. However, the precise measurement of  $\tau_c$  suffers from the gradual transitions in the photocurrent from  $I_{ph} \propto t^{-(1-\alpha)}$  to  $I_{ph} \propto t^{-(1+\alpha)}$ . In addition, it has been shown that the thermalization approximation does not work for structured distributions of localized tail states [3] and for exponential band tail states whose width is smaller than  $kT$ , where  $kT$  is the thermal energy. Information on  $\tau_R$  is important for the understanding of nature of recombination centers in amorphous semiconductors. Since the transient photocurrent is intimately related to the energetic distribution of localized states and  $\tau_R$ , it may be used to study them, and various techniques have been advanced for doing so [4-6]. The DOS and  $\tau_R$  are key material quality indicators, of importance in the design of improved solar cells, photodetectors and thin-film transistors. A simple and reliable method is introduced to evaluate  $\tau_R$ .

We develop in this paper a new method for measuring  $\tau_R$  and DOS  $g(E)$  in disordered semiconductors from an experimental transient photocurrent data. The present method consists of three steps: first,  $\tau_R$  is estimated from the experimental TPC data using Laplace



transform technique. Secondly, exact DOS  $g(E)$  is determined from the same experimental TPC data using the same Laplace transform technique [7-10]. Thirdly, computer-generated transient photocurrent using the calculated  $\tau_R$  and DOS  $g(E)$  must reproduce the experimental one, and thus to valid the method. The method is applied to the study of the effects of random noise and truncated data on  $\tau_R$  for simulated TPC on the one hand and the effect of temperature on  $\tau_R$  in undoped a-Si: H sample on the other hand.

## 2. Theory

### 2.1. Recombination lifetime determination

In the TPC technique, the transient photocurrent is determined by the time dependence of the photoconductivity following carrier excitation by means of a short pulse of illumination in samples having a coplanar electrode configuration [2]. For the theoretical analysis of this measurement, it suits to assume unipolar conduction, equal capture cross section for all localized states and small signal condition (the injected charge density is low enough that the localized states are not saturated and that the internal electric field is not perturbed) [7]. The small signal condition ensures the monomolecular recombination kinetics of photogenerated carriers and avoids space charge effects. We assume the transient photocurrent is carried solely by carriers in extend states, which interact through trapping and release with a distribution of localized states. Then, the basic linearized multiple trapping equations for free and trapped electrons respectively are:

$$\frac{dn(t)}{dt} = -\sum_i \frac{dn_i(t)}{dt} - \frac{n(t)}{\tau_R} + N_0 \delta(t), \quad (1)$$

$$\frac{dn_i(t)}{dt} = \omega_i n(t) - \gamma_i n_i(t), \quad (2)$$

where  $n(t)$  is the free carrier density at time  $t$ ,  $n_i(t)$  the trapped carrier density at the  $i^{th}$  localized state at time  $t$ ,  $N_0$  the pulsed electron density (the excess free electron density at

the initial time  $t = 0$ ),  $\tau_R$  the recombination lifetime,  $\omega_i = \sigma v g(E_i) \Delta E$  the capture rate constant,  $\gamma_i = \nu \exp\left(\frac{-E_i}{kT}\right)$  the release rate constant,  $E_i = i\Delta E$  the  $i^{\text{th}}$  energy level below (or above) a mobility edge,  $\sigma$  the capture cross section,  $v$  the thermal velocity and  $\nu$  the attempt-to-escape frequency. The delta function in Eq. (1) defines the initial condition for the transient photoconductivity experiment. We set the conduction band mobility edge at  $E_c = 0$ , so that  $E$  is negative.

Eqs. (1) and (2) may be solved to yield the Laplace transform of the free carrier density  $n(t)$ . The Laplace transform of  $n(t)$  is defined as:

$$\hat{n}(s) = \int_0^{\infty} n(t) e^{-st} dt$$

The solution of Eqs. (1) and (2) for  $\hat{n}(s)$  is:

$$\hat{n}(s) = \frac{N_0}{s + \frac{1}{\tau_R} + \sum_i \frac{s\omega_i}{s + \gamma_i}}, \quad (3)$$

that is to say

$$\frac{1}{\tau_R} = \frac{N_0}{\hat{n}(s)} - s \left( 1 + \sum_i \frac{\omega_i}{s + \gamma_i} \right), \quad (4)$$

in which  $s$  is the Laplace variable.

For the TPC experiment, the photocurrent is given by  $I(t) = q\mu_0 F S n(t)$ , where  $q$  is the electron charge,  $\mu_0$  the microscopic mobility,  $F$  the applied electric field and  $S$  the conduction cross section, which is transformed into

$$\hat{I}(s) = q\mu_0 F S \hat{n}(s). \quad (5)$$

Inserting Eq. (5) into Eq. (4), one obtains

$$\frac{1}{\tau_R} = \frac{q\mu_0 F S N_0}{\hat{I}(s)} - s \left( 1 + \sum_i \frac{\omega_i}{s + \gamma_i} \right), \quad (6)$$

for  $s = 0$  one obtains

$$\tau_R = \frac{\hat{I}(0)}{I(0)} = \frac{\int_0^{\infty} I(t) dt}{I(0)}, \quad (7)$$

where  $I(0) = q\mu_0 FSN_0$ , which is estimated from the extrapolated value of  $I(t)$  to  $t = 0$ .

$\hat{I}(0)$  can be carried out by a simple numerical integration over  $N$  sampling points  $t_j$ :

$$\hat{I}(0) = \sum_{j=2}^{N-1} I(t_j) \Delta t_j, \quad (8)$$

where  $\Delta t_j = \frac{t_{j+1} - t_{j-1}}{2}$ .

Eq. (7) is a simple and adequate relationship that leads to the estimate of  $\tau_R$ . Like one see  $\tau_R$  depends only on experimental  $I(t)$  data and initial photocurrent  $I(0)$ , i.e. generated excess density  $N_0$ .

To investigate the potential accuracy of the  $\tau_R$  determination procedure, it is necessary to simulate accurately the transient photocurrent for the following two representative localized state distributions in amorphous and polymeric semiconductors: (i) an exponential distribution

$g(E) = g(E_c) \exp\left(\frac{-E}{kT_c}\right)$  and (ii) an exponential distribution on which a Gaussian distribution

has been superimposed  $g(E) = g(E_c) \exp\left(\frac{E}{kT_c}\right) + g_g \exp\left[-\left(\frac{E - E_g}{E_w}\right)^2\right]$ , where  $g(E_c)$  is the

density of localized states at the mobility edge,  $T_c$  the characteristic temperature and  $g_g$ ,  $E_g$  and  $E_w$  the peak value, the energy position from the mobility edge and the energy width of the Gaussian distribution, respectively.

In the present work  $n(t)$  was carried out by means of an analytical expression for the inverse Laplace transform of  $\hat{n}(s)$ , obtained from Eq. (3), using Heaviside's expansion theorem [11].

$$n(t) = L^{-1}\{\hat{n}(s)\} = \sum_{i=1}^{n+1} \frac{P(\alpha_i)}{Q'(\alpha_i)} e^{\alpha_i t}, \quad (9)$$

In Eq. (9) the  $\alpha_i$  are the  $n+1$  zeroes of the denominator  $Q(s)$  and  $Q'(\alpha_i)$  is the first derivative of  $Q(s)$  taken at points  $\alpha_i$ .  $\hat{n}(s)$  is of the form of  $\frac{P(s)}{Q(s)}$ .

Fig. 1b shows the TPC,  $n(t)$ , computed at 300K for the proposed exponential DOS model of Fig. 1a with various values of  $\tau_R$ . The inflection points in the transients are due to the monomolecular recombination of the photogenerated free carriers. The characteristic recombination time determined from the inflection point,  $\tau_c$ , is much larger than  $\tau_R$ , this results from frequent trapping and detrapping of free carriers into the exponential localized-state distributions. The value of  $\tau_c$  increases with  $\tau_R$ . The  $\tau_R$  used in the simulation of  $n(t)$ , are, respectively,  $10^{-8}$ ,  $10^{-7}$  and  $10^{-6}$  s. The corresponding calculated  $\tau_R$  using Eq. (7) are, respectively,  $9.0165 \times 10^{-9}$ ,  $8.8164 \times 10^{-8}$  and  $8.7647 \times 10^{-7}$  s. It can be seen that the introduced  $\tau_R$  were recovered with high accuracy.

Fig. 2b shows the TPC,  $n(t)$ , computed at 350K for the proposed exponential plus Gaussian DOS model of Fig. 2a with  $\tau_R = 10^{-8}$  s. As in the case of computed TPC,  $n(t)$ , for an exponential DOS model, one can see well the inflection point in the transient due to recombination. The corresponding calculated  $\tau_R$  using Eq. (7) is  $8.7256 \times 10^{-9}$  s. It can be seen here also that the proposed method recovers very precisely the introduced  $\tau_R$ .

Figs. 3a, 3b, 3c and 4 show the TPC,  $n(t)$  (symbol), of Figs. 1b ( $\tau_R = 10^{-6}, 10^{-7}, 10^{-8}$  s) and 2b respectively, and  $\tau_R(s^{-1})$  (solid line) for corresponding  $\hat{n}(s)$  (Eq. (4)). One can see that  $\tau_R(s^{-1})$  remains constant till the characteristic recombination time  $\tau_c$  and equal to introduced value of  $\tau_R$  in the simulation of  $n(t)$ . Normally  $\tau_R$  is independent of  $s$ , but most important is that  $\tau_R(s^{-1})$  is constant and equal to introduced  $\tau_R$  for small values of  $s$  and for

1  
2  
3  
4  
5  
6  
7  
8  
9  
10  
11  
12  
13  
14  
15  
16  
17  
18  
19  
20  
21  
22  
23  
24  
25  
26  
27  
28  
29  
30  
31  
32  
33  
34  
35  
36  
37  
38  
39  
40  
41  
42  
43  
44  
45  
46  
47  
48  
49  
50  
51  
52  
53  
54  
55  
56  
57  
58  
59  
60

$s = 0$  also of course (Eq. (7)). An important observation, the curve  $\tau_R(s^{-1})$  deviates from introduced  $\tau_R$  exactly at the moment when recombination begins, the curves  $n(t)$  and  $\tau_R(s^{-1})$  intersect at this specific time. Which means that the proposed method is not valid when the recombination phenomenon is not observed, this happens for low temperatures of measurement of  $n(t)$ , at short times.

## 2.2. Density of localized states

Eq. (6) can also be written as follows:

$$\sum_i \frac{g(E_i)}{s + \gamma_i} = \frac{1}{s \sigma v \Delta E} \left( \frac{q \mu_0 F S N_0}{\hat{I}(s)} - s - \frac{1}{\tau_R} \right), \quad (10)$$

We note here  $\tau_R$  is experimentally known (Eq. (7)).

Eq. (10) is an integro-differential equation for the DOS  $g(E)$ , termed a Fredholm integral equation of the first kind [12] which may arise from an ‘ill-conditioned problem’. The inversion of this equation to obtain the DOS requires care, it needs a special resolution method. The resolution method used here is an exact matrix solution for  $g(E)$  based on Tikhonov regularization [13,14]. Written in a discrete form, Eq. (10) yields

$$\sum_{i=1}^M g(i) A(j, i) = b(j) \quad \text{for } j = 2, \dots, N-1, \quad (11)$$

where  $i$  and  $j$  are the energy and time indexes respectively, and  $g(i) = g(E_i)$ . The matrix elements  $A(j, i)$  and the vector elements  $b(j)$  are respectively,

$$A(j, i) = \frac{1}{s(j) + \gamma(i)},$$

$$b(j) = \frac{1}{s(j) \sigma v \Delta E} \left( \frac{q \mu_0 F S N_0}{\hat{I}(j)} - s(j) - \frac{1}{\tau_R} \right),$$

where  $\gamma(i) = \nu \exp\left(\frac{-E_i}{kT}\right)$ ,  $s(j) = \frac{1}{t_j}$  and  $\hat{I}(j) = \hat{I}(s_j)$ .

The DOS vector is then given by

$$g = A^{-1}b. \quad (12)$$

This expression constitutes the basis of the transient method that returns for  $\hat{I}(j)$  (i.e. the TPC data) a DOS distribution  $g(E)$  of localized states.

### 3. Experiment

#### 3.1. Preparation of sample

[15] A P-doped sample of a-Si:H was prepared by RF glow discharge decomposition of  $\text{SiH}_4$  with 3 vppm  $\text{PH}_3$ . Coplanar Al electrodes of 0.5 mm gap and 5 mm width were deposited on top of the film of 1  $\mu\text{m}$  thickness, and the voltage applied across the gap was 400 V (i.e. an electric field of 8000  $\text{Vcm}^{-1}$ ). The light source employed was a Laser Science VSL337  $\text{N}_2$ -pumped 5 ns pulse dye laser, 640 nm, producing pulsed carrier densities of up to  $10^{20} \text{ cm}^{-3}$ , varied by means of neutral density filters. Single shots or low frequency ( $\ll 1\text{Hz}$ ) laser pulses were used to allow complete carrier relaxation. The TPC signal was amplified where necessary, and measured using a PC-controlled Tektronix TDS380 oscilloscope as a transient recorder. A temperature range from 120–400 K was covered using a cryostat operating at a chamber pressure of typically  $10^{-4}$  Torr. The dark Fermi level was estimated from the dark conductivity measurement to be 0.5 eV below the conduction band mobility edge.

#### 3.2. Results

In the following, the free carriers lifetime  $\tau_R$  and the energy profile of the DOS  $g(E)$  are determined from an experimental TPC data. TPC are then generated by numerical simulation, using these  $\tau_R$  and DOS, and compared to the experimental ones.

Fig. 5 shows a set of five TPC decays for the P-doped a-Si:H sample at 150, 200, 250, 290 and 310 K measured with an excitation density of  $N_0 = 10^{16} \text{ cm}^{-3}$ .

To valid the proposed method for the experimental case, we determinate  $\tau_R$  and exact DOS  $g(E)$  from the experimental TPC data of Fig. 5. We then simulate TPC using these  $\tau_R$  and DOS  $g(E)$  in order to reproduce the experimental ones. Using Eq. (7) for measured TPC decays at 200, 250 and 310K of Fig. 5, we find respectively the following values of  $\tau_R$ :  $1.2933 \times 10^{-6}$  s,  $9.7965 \times 10^{-7}$  s and  $8.552 \times 10^{-7}$  s. And by inserting these values of  $\tau_R$  into Eq. (10) for each case (200, 250 and 310K), we determine the energy profile of the DOS  $g(E)$  after calculating the corresponding  $\hat{I}(s)$  (Eq. (5)).

Fig. 6 shows the portion DOS  $g(E)$ , calculated by the inversion of Eq. (10), in the P-doped sample of Fig. 5 for the temperatures 200, 250 and 310K. The solid line is the DOS model obtained by fitting of the experimental DOS to the DOS expression:

$$g(E) = g(E_c) \exp\left(\frac{E}{kT_{c1}}\right) \left[ 1 - \frac{1}{1 + \exp\left(\frac{E - E_d}{kT_{c2}}\right)} \right] + g_g \exp\left[-\left(\frac{E - E_g}{E_w}\right)^2\right]. \quad (13)$$

Equation (13) indicates that the DOS model presents two exponential distributions parts on which a Gaussian distribution has been superimposed. One exponential distribution above  $E_d$  with high characteristic temperature  $T_{c1}$  and the other below  $E_d$  with low characteristic temperature  $T_c = \frac{T_{c1}T_{c2}}{T_{c1} + T_{c2}}$ . Least squares fitting gives  $g(E_c) = 3.2279 \times 10^{21} \text{ cm}^{-3} \text{ eV}^{-1}$ ,

$E_d = 0.12417 \text{ eV}$  below  $E_c$ ,  $T_{c1} = 1321.3 \text{ K}$  and  $T_{c2} = 211.49 \text{ K}$ , resulting in  $T_c \approx 182.3 \text{ K}$ .

For the Gaussian distribution,  $g_g = 3.1292 \times 10^{15} \text{ cm}^{-3} \text{ eV}^{-1}$ ,  $E_g = 0.36888 \text{ eV}$  below  $E_c$  and  $E_w = 29.685 \text{ meV}$ . The result is a well-defined step exponential conduction band tail of characteristic temperature  $T_c$  with a slight deviation towards  $E_c$  at the top to which is added a Gaussian distribution of energy width  $E_w$  and whose the peak, of value  $g_g$ , is positioned at  $E_g$  below the mobility edge  $E_c$ . The doping effect on the tail shape is remarkable, the DOS

with energies around the donor (P) band peak at a certain level  $E_d$  between 0.1eV and 0.2eV below  $E_c$  [16] is found to increase with doping. The DOS is then, a broad distribution above  $E_d$ , a narrow tail below it and a deeper Gaussian distribution, so that the DOS profile can be fitted with the DOS model of Eq. (13).

The parameters used to perform  $\tau_R$  and the DOS  $g(E)$  are the following:

$$\mu_0 = 10 \text{ cm}^2 \text{ s}^{-1} \text{ V}^{-1}, C_n = \sigma \nu = 2 \times 10^{-8} \text{ cm}^3 \text{ s}^{-1} \text{ and } \nu = 10^{12} \text{ s}^{-1}.$$

Fig. 7 shows the computed TPC decays (solid lines) for the P-doped sample at temperatures 200, 250 and 310K using the DOS model of Fig. 6. The corresponding experimental TPC decays of Fig. 5 are also presented (symbols). It turns out that, the modelled TPC curves line up quite rigorously with the experimental ones.

## 4. Discussion

### 4.1. Temperature effect

Limitations of the method are essentially the effect of low temperatures of TPC measurement on  $\tau_R$  when the recombination phenomenon is not observed at short times. Fig.

9 shows the TPC,  $n(t)$ , computed at 150K between initial time  $t_i = \frac{1}{\nu}$  and various values of

final time  $t_f = \frac{1}{\nu} \exp\left(\frac{E_c - E}{kT}\right)$  for the proposed exponential plus Gaussian DOS model of Fig.

8 with  $\tau_R = 10^{-8}$  s. The chosen  $t_f$  are, respectively, 1,  $10^2$  and  $10^4$  s. The corresponding

calculated  $\tau_R$  using Eq. (7) are, respectively,  $2.9693 \times 10^{-9}$ ,  $9.8854 \times 10^{-8}$  and  $7.3038 \times 10^{-7}$  s.

It can be seen here that the proposed method does not recovers the introduced  $\tau_R$ . We can

retrieve the 'exact' value of the pre-proposed  $\tau_R$  for low temperatures, provided to take

extremely long times, which is not feasible experimentally. In conclusion we can say that the

method is influenced by the temperature, it is valid only when the phenomenon of



1 recombination is observable, that is to say in the case of high temperatures. Higher  
2 temperature is better, as it shifts the recombination feature to shorter times, into the accessible  
3 time-region. Therefore, at low temperatures there is a little evidence of the effect of  
4 recombination on TPC over the experimental timescale.  
5  
6  
7  
8  
9

#### 10 4.2. Truncated data

11  
12 Fig. 10 shows the TPC,  $n(t)$  (solid line), computed at 350 K between initial time  $t_i = 1$  ps  
13 and final time  $t_f = 1$  s for the proposed exponential plus Gaussian DOS model of Fig. 2a with  
14  $\tau_R = 10^{-8}$  s and the truncated  $n(t)$  (symbol o) at time 10 ns after  $t_i$ , i.e. 10 ns is the new  
15 starting time  $t_i$ . For the full data  $n(t)$ ,  $\tau_R$  was already been calculated (section 2.1), it is  
16 worth  $8.7256 \times 10^{-9}$  s and for the truncated one,  $\tau_R$  is equal to  $8.5912 \times 10^{-9}$  s, it was  
17 calculated in the same way as in the case of complete data (Eq. 7). Fig. 11 shows the same full  
18 TPC,  $n(t)$  (solid line) as of Fig. 10 and the truncated  $n(t)$  (symbol o) at time  $100 \mu$ s before  
19  $t_f$ , i.e.  $100 \mu$ s is the new final time  $t_f$ . For the truncated one,  $\tau_R$  is equal to  $8.7217 \times 10^{-9}$  s.  
20  
21 As we see the estimation of  $\tau_R$  is not influenced by the missing of short or long-time data.  
22  
23 This implies that there must be some influence of recombination at short times, long before  
24 the 'final' recombination decay which we normally expect (and see) at long times.  
25  
26  
27  
28  
29  
30  
31  
32  
33  
34  
35  
36  
37  
38

#### 39 4.3. Noisy data

40  
41 Accuracy of measuring  $\tau_R$  has been already investigated by application to simulated  
42 (perfect) data, but how good is it when used on real (imperfect) data, subject to noise? To do  
43 this, we simulate TPC,  $n(t)$ , for given DOS model and  $\tau_R$ , and add Gaussian noise whose  
44 amplitude is a constant fraction of  $n(t)$ . Random noise is approximately Gaussian of similar  
45 amplitude over whole time range. Noise was introduced by multiplying each point of  $n(t)$  by  
46 a random number from a Gaussian distribution whose mean value is 1. The standard deviation  
47 of the distribution was varied between 10% and 40%.  
48  
49  
50  
51  
52  
53  
54  
55  
56  
57  
58  
59  
60

1  
2 Fig. 12 shows the simulated (smoothed) TPC,  $n(t)$  (solid line), of Fig. 2b and the noisy  
3  
4  $n(t)$  (symbol o) when noise level is equal to 10%. Eq. (7) gives  $\tau_R = 8.7256 \times 10^{-9}$  s for  
5  
6 simulated  $n(t)$  and  $9.0484 \times 10^{-9}$  s for noisy  $n(t)$  when the used  $\tau_R$  in the simulation of  $n(t)$   
7  
8 is  $10^{-8}$  s. It can be seen that the estimation of  $\tau_R$  is not influenced by noise.  
9  
10

11 Fig. 13 shows the deviation  $\frac{\text{smoothed data} - \text{noisy data}}{\text{smoothed data}}$  versus time in the case of 10%  
12  
13 noise. As we see Gaussian noise is approximately uniform over entire time range.  
14  
15

16 Fig. 14 shows estimated  $\tau_R$  versus noise level, this last varying between 10% and 40%.  
17  
18  $\tau_R$  remains practically constant, and equal to  $10^{-8}$  s, over whole noise level range. The  
19  
20 method is 'noise tolerant', it is capable of returning optimal resolution for a given set of noisy  
21  
22 data even at quite high input noise levels.  
23  
24  
25  
26  
27  
28  
29  
30  
31  
32  
33  
34  
35  
36  
37  
38  
39  
40  
41  
42  
43  
44  
45  
46  
47  
48  
49  
50  
51  
52  
53  
54  
55  
56  
57  
58  
59  
60

## 5. Conclusion

We have proposed a new method for determining the free carriers lifetime  $\tau_R$  and the density of localized states DOS in amorphous semiconductors from the transient photocurrent TPC data. This technique involves Laplace transform of TPC data, it is a simple analysis of the solution of the basic linearized multiple trapping equations for free and trapped electrons. It has been tested by applying it to simulated and experimental TPC data measured on a typical disordered semiconductor, the hydrogenated amorphous silicon (a-Si:H). An introduced  $\tau_R$  in the computing of the TPC using an arbitrarily proposed DOS model is recovered with high accuracy. For the experimental case, the estimated  $\tau_R$  and the determination of the exact DOS from the experimental TPC data allow to reconstruct accurately this last. Limitations of the technique are essentially the effect of low temperatures of TPC measurement on  $\tau_R$  when the recombination phenomenon is not observed at short times. On the other hand, the determination of  $\tau_R$  is not at all influenced by the missing of short or long-time data and the noisy data.

**Acknowledgements**

The authors thank Amorphous Semiconductors group at Dundee University for the measurement facilities. The Algerian Ministry of Higher Education and Research is acknowledged for his financial support.

For Peer Review Only

**References**

- [1] R.H. Bube, Photoelectric properties of semiconductors, Cambridge University Press, Cambridge, 1992.
- [2] J. Orenstein, M.A. Kastner, and V. Vaninov, **Transient photoconductivity and photo-induced optical absorption in amorphous semiconductors**, Philos. Mag. B 46 (1982) pp. 23-62.
- [3] G. Seynhaeve, G.J. Adriaenssens, and H. Michiel, **On the density of localized states obtainable from transient photodecay measurements**, Solid State Commun. 56 (1985) pp. 323-326.
- [4] G.J. Adriaenssens, S.D. Baranovskii, W. Fuhs, J. Jansen, and Ö. Öktü, **Photoconductivity response time in amorphous semiconductors**, Phys. Rev. B 51 (1995) pp. 9661-9667.
- [5] T. Nagase, and H. Naito, **Determination of free carrier recombination lifetime in amorphous semiconductors: Application to the study of iodine doping effect in arsenic triselenide**, J. Non-Cryst. Solids 227-230 (1998) pp. 824-828.
- [6] R.R. Koropecski, J.A. Schmidt, and R. Arce, **Density of states in the gap of amorphous semiconductors determined from modulated photocurrent measurements in the recombination regime**, J. Appl. Phys. 91 (2002) pp. 8965-8969.
- [7] H. Naito, J. Ding, and M. Okuda, **Determination of localized state distributions in amorphous semiconductors from transient photoconductivity**, Appl. Phys. Lett. 64 (1994) p. 1830.
- [8] H. Naito, and M. Okuda, **Simple analysis of transient photoconductivity for determination of localized state distributions in amorphous semiconductors using Laplace transform**, J. Appl. Phys. 77 (1995) p. 3541.
- [9] H. Naito, T. Nagase, T. Ishii, M. Okuda, T. Kawaguchi, and S. Maruno, **Density of states in amorphous semiconductors determined from transient photoconductivity experiment: Computer simulation and experiment**, J. Non-Cryst. Solids 198-200 (1996) pp. 363-366.

- 1  
2  
3  
4  
5  
6  
7  
8  
9  
10  
11  
12  
13  
14  
15  
16  
17  
18  
19  
20  
21  
22  
23  
24  
25  
26  
27  
28  
29  
30  
31  
32  
33  
34  
35  
36  
37  
38  
39  
40  
41  
42  
43  
44  
45  
46  
47  
48  
49  
50  
51  
52  
53  
54  
55  
56  
57  
58  
59  
60
- [10] N. Ogawa, T. Nagase, and H. Naito, **Improvement of energy resolution of transient photoconductivity analysis for measuring localized-state distributions in amorphous semiconductors**, *J. Non-Cryst. Solids* 266-269 (2000) pp. 367-371.
- [11] M.R. Spiegel, *Schaum's outline of theory and problems of Laplace transforms*, McGraw-Hill, 1965.
- [12] T. Nagase, K. Kishimoto, and H. Naito, **High resolution measurement of localized-state distributions from transient photoconductivity in amorphous and polymeric semiconductors**, *J. Appl. Phys.* 86 (1999) pp. 5026-5035.
- [13] A.N. Tikhonov, A.V. Goncharsky, V.V. Stepanov, and A.G. Yagola, *Numerical Methods for the Solution of ill-Posed Problems*, Kluwer, Dordrecht, 1995.
- [14] J. Weese, **A reliable and fast method for the solution of Fredhol integral equations of the first kind based on Tikhonov regularization**, *Comput. Phys. Commun.* 69 (1992) pp. 99-111.
- [15] A. Merazga, A.F. Meftah, A.M. Meftah, C. Main, and S. Reynolds, **Defect pool model based transient photoconductivity and the conduction band tail profile in a-Si:H**, *J. Phys.: Condens. Matter* 13 (2001) pp. 10969-10977.
- [16] R.A. Street, *Hydrogenated Amorphous Silicon*, Cambridge University Press, Cambridge, 1991.